A posteriori error analysis of an augmented mixed method for the Navier-Stokes equations with nonlinear viscosity *

Gabriel N. Gatica[†], Ricardo Ruiz-Baier[‡], Giordano Tierra[§]

Abstract

In this work we develop the a posteriori error analysis of an augmented mixed finite element method for the 2D and 3D versions of the Navier-Stokes equations when the viscosity depends nonlinearly on the module of the velocity gradient. Two different reliable and efficient residual-based a posteriori error estimators for this problem on arbitrary (convex or non-convex) polygonal and polyhedral regions are derived. Our analysis of reliability of the proposed estimators draws mainly upon the global inf-sup condition satisfied by a suitable linearization of the continuous formulation, an application of Helmholtz decomposition, and the local approximation properties of the Raviart-Thomas and Clément interpolation operators. In addition, differently from previous approaches for augmented mixed formulations, the boundedness of the Clément operator plays now an interesting role in the reliability estimate. On the other hand, inverse and discrete inequalities, and the localization technique based on triangle-bubble and edge-bubble functions are utilized to show their efficiency. Finally, several numerical results are provided to illustrate the good performance of the augmented mixed method, to confirm the aforementioned properties of the a posteriori error estimators, and to show the behaviour of the associated adaptive algorithm.

1 Introduction

In the recent work [11], a new dual-mixed finite element method for the Navier-Stokes equations with constant density and variable viscosity – depending nonlinearly on the gradient of velocity – has been introduced and analyzed. More precisely, the approach in [11] employs a technique previously applied to the Navier-Stokes equations with constant viscosity (see [12] and [32]), which is based on the introduction of a modified pseudostress tensor involving the diffusive and convective terms, and the pressure. The latter is then eliminated thanks to the incompressibility condition, and the nonlinear viscosity is handled by incorporating the gradient of velocity as an auxiliary tensor unknown. In addition, the fact that the convective term forces the velocity to live in a smaller space motivates the augmentation of the variational formulation with suitable penalty terms arising mainly from the constitutive and equilibrium equations, and the relation defining the aforementioned gradient. As a consequence, the resulting augmented scheme can be written equivalently as a fixed point equation,

*This research was partially supported by BASAL project CMM, Universidad de Chile, by Centro de Investigación en Ingeniería Matemática (CI^{2}MA), Universidad de Concepción, by CONICYT project Anillo ACT1118 (ANANUM), by the Swiss National Science Foundation through the research grant SNSF PP00P2-144922, by the Elsevier Mathematical Sciences Sponsorship Fund (MSSF), and by the Ministry of Education, Youth and Sports of the Czech Republic through the ERC-CZ project LL1202.

[†]CI^{2}MA and Departamento de Ingeniería Matemática, Universidad de Concepción, Casilla 160-C, Concepción, Chile, email: ggatica@ci2ma.udec.cl

[‡]Mathematical Institute, University of Oxford, A. Wiles Building, Radcliffe Observatory Quarter, Woodstock Road, Oxford OX2 6GG, United Kingdom, email: ruizbaier@maths.ox.ac.uk

[§]Department of Mathematics, Temple University, Philadelphia, PA 19122, USA, e-mail: gtierra@temple.edu

and hence the well-known Schauder and Banach theorems, together with classical results on monotone operators, yield the well-posedness of the continuous and discrete systems. In particular, the usual discrete inf-sup conditions are not required anymore, and therefore the unique solvability of the Galerkin scheme is guaranteed with arbitrary finite element subspaces of the respective continuous spaces.

The purpose of the present paper is to develop a residual-based a posteriori error analysis for the problem and method from [11]. Regarding this goal, we begin by remarking that standard Galerkin procedures such as finite element and mixed finite element methods inevitably lose accuracy when applied to nonlinear problems on quasi-uniform discretisations. The main reason for this fact is that, in general, no a priori hints on how to mesh the domains are available in these cases, and hence one normally employs adaptive algorithms that are based on a posteriori error estimates. While the list of references on a posteriori error analysis for linear and nonlinear problems is nowadays quite extensive, and includes some important contributions in recent years, some of which are mentioned in what follows, it is important to remark that most of the main ideas and associated techniques can be found in the early works [3], [38] and the references therein.

Now, aiming at as complete as possible bibliographic discussion on the main topics involved in this paper, we refer first to [34] and [35], where reliable a posteriori error estimates for finite element approximations of primal variational formulations of the compressible Euler and Navier-Stokes equations have been developed. The main tools utilized there include the element residual method and the introduction of a special norm to measure the error in the velocity and pressure. Further contributions in this direction for the steady incompressible Navier-Stokes equations are found in [6] and [8], where an abstract estimate yielding Hood-Taylor and modified Hood-Taylor finite element as particular examples, and the Becker-Rannacher "*dual-weighted-residual method*" for optimal-control problems, are employed, respectively. Other related works dealing with the classical velocity-pressure formulation of the steady incompressible Navier-Stokes equations include [39], [37], and [33]. In particular, residual type a posteriori error estimates for a stabilised finite element method are developed in [33] by applying a general framework established by Verfürth for nonlinear equations. Moreover, a simple error estimator in $\mathrm{L}^2 - \mathrm{L}^2$ norm is also presented in [33] by using a duality argument. Furthermore, a posteriori error analysis for discontinuous Galerkin approximations of the Navier-Stokes equations are developed in [30] and [31]. More precisely, a duality argument of weighted type is applied in [30] to derive a posteriori bounds and an adaptive mesh design for the interior penalty discontinuous Galerkin finite element approximation of the compressible Navier-Stokes equations. In turn, upper and lower bounds for the velocity-pressure error measured in terms of the energy norm of the discretisation for the two-dimensional stationary incompressible Navier-Stokes equations (in the case of small data) are obtained in [31]. On the other hand, a number of dual mixed approaches for the Navier-Stokes equations and the derivation of corresponding a posteriori error estimates, have begun to appear only in the last decade in the literature. For instance, we can refer to [20] where quasi-optimal a priori estimates and a posteriori error estimates for a mixed finite element approximation of this system in a polygonal domain of the plane are provided. Dirichlet boundary conditions for the velocity and the velocity gradient as an additional unknown are considered in [20]. In addition, the main tools for the a posteriori error analysis developed there include an abstract nonlinear theory and the posteriori error estimates for the Stokes equations from [19]. Other contributions in this direction include [26], [27], and the already mentioned work [32], which, as explained above, suggested one of the techniques employed in [11], which, in turn, motivated the present paper. Concerning the aforementioned references, we remark that the key aspects of the analysis in [27], which deals with a velocity-pseudostress approach for a class of quasi-Newtonian Stokes flows, are a global inf-sup condition for a linearised version of the resulting nonlinear twofold saddle point operator equation, and a conveniently constructed Helmholtz

decomposition of the space containing the stresses of the fluid, together with its discrete counterpart. The technique from [27] was then extended in [21] to any nonlinear twofold saddle point variational formulation. Nevertheless, irrespective of it, and as we show below in the present paper, the approach from [27] and [21] can also be applied to other nonlinear problems not showing a twofold saddle point structure. Finally, and just for sake of completeness, we mention that a posteriori error estimates for mixed finite element discretisations of the evolutionary Navier-Stokes equations are derived in [10] and [16], and that an a posteriori error analysis for an iterative algorithm solving Navier-Stokes has been proposed very recently in [9].

According to the above discussion, in this paper we adapt the strategy proposed in [27] and [21] to derive reliable and efficient residual-based a posteriori error estimators for the model and augmented mixed method introduced in [11]. This means that our analysis begins with a global inf-sup condition for the linearisation arising from the use of the Gâteaux derivatives of the nonlinear terms of the formulation. Then, our remaining tools include a suitable handling of the corresponding convective term of the Navier-Stokes equations, continuous and discrete Helmholtz's decompositions, local approximation properties of the Raviart-Thomas and Clément interpolation operators, inverse inequalities, and the localization technique based on triangle-bubble and edge-bubble functions. The rest of the work is organised in the following manner. Both strong and weak forms of the velocity gradient-stress-velocity formulation of the Navier-Stokes equations with nonlinear viscosity are stated in Section 2. We recall the main hypotheses on the viscosity nonlinearity and define a Galerkin scheme, detailing a particular choice of the discrete spaces and stating the a priori error bounds established in [11]. Next, in Section 3 we consider the 2D case, introduce two a posteriori error indicators, and derive the corresponding theoretical bounds yielding reliability and efficiency of each estimator. The analysis and results from Section 3 are then extended to the 3D case in Section 4. Finally, in Section 5 we collect several numerical examples illustrating the good performance and good effectivity indexes of both error estimators under diverse scenarios in 2D and 3D, and confirming the satisfactory behaviour of the corresponding adaptive refinement strategies.

2 The Navier–Stokes equations with nonlinear viscosity

2.1 Preliminaries

Let us denote by $\Omega \subseteq \mathbb{R}^n$, $n \in \{2,3\}$, a given open, bounded, and connected domain with polygonal (polyhedral) boundary Γ, and denote by $\boldsymbol{\nu}$ the outward unit normal vector on Γ. Standard notation will be adopted for Lebesgue spaces $\mathrm{L}^p(\Omega)$ and Sobolev spaces $\mathrm{H}^s(\Omega)$ with norm $\|\cdot\|_{s,\Omega}$ and seminorm $|\cdot|_{s,\Omega}$. In addition, by $\mathbf{M}$ and $\mathbb{M}$ we will refer to the corresponding vector and tensorial counterparts of the generic scalar functional space M, whereas $\|\cdot\|$, with no subscripts, will stand for the natural norm of either an element or an operator in any product functional space. On the other hand, for any vector fields $\boldsymbol{v} = (v_i)_{i=1,n}$ and $\boldsymbol{w} = (w_i)_{i=1,n}$, we set the gradient, divergence, and tensor product operators, as

$$\nabla \boldsymbol{v} := \left(\frac{\partial v_i}{\partial x_j} \right)_{i,j=1,n}, \quad \mathrm{div}\, \boldsymbol{v} := \sum_{j=1}^{n} \frac{\partial v_j}{\partial x_j}, \quad \text{and} \quad \boldsymbol{v} \otimes \boldsymbol{w} := (v_i\, w_j)_{i,j=1,n}\,.$$

Furthermore, for any tensor fields $\boldsymbol{\tau} = (\tau_{ij})_{i,j=1,n}$ and $\boldsymbol{\zeta} = (\zeta_{ij})_{i,j=1,n}$, we let $\mathbf{div}\, \boldsymbol{\tau}$ be the divergence operator div acting along the rows of $\boldsymbol{\tau}$, and define the transpose, the trace, the tensor inner product, and the deviatoric tensor, respectively, as

$$\boldsymbol{\tau}^{\mathtt{t}} := (\tau_{ji})_{i,j=1,n}, \quad \mathrm{tr}(\boldsymbol{\tau}) := \sum_{i=1}^{n} \tau_{ii}, \quad \boldsymbol{\tau} : \boldsymbol{\zeta} := \sum_{i,j=1}^{n} \tau_{ij}\zeta_{ij}\,, \quad \text{and} \quad \boldsymbol{\tau}^{\mathtt{d}} := \boldsymbol{\tau} - \frac{1}{n}\,\mathrm{tr}(\boldsymbol{\tau})\,\mathbb{I}\,.$$

Finally, we define the following tensorial functional spaces:

$$\mathbb{H}_0(\mathbf{div};\Omega) := \left\{ \boldsymbol{\zeta} \in \mathbb{H}(\mathbf{div};\Omega) : \quad \int_\Omega \mathrm{tr}(\boldsymbol{\zeta}) = 0 \right\},$$

and

$$\mathbb{L}^2_{\mathtt{tr}}(\Omega) := \left\{ \boldsymbol{s} \in \mathbb{L}^2(\Omega) : \quad \mathrm{tr}\,\boldsymbol{s} = 0 \right\}.$$

2.2 The boundary value problem

We consider the stationary Navier-Stokes equations with nonlinear viscosity, that is

$$\begin{aligned} -\,\mathbf{div}\big(\mu(|\nabla \boldsymbol{u}|)\,\nabla \boldsymbol{u}\big) + \boldsymbol{u}\cdot\nabla\boldsymbol{u} + \nabla p &= \boldsymbol{f} \quad \text{in} \quad \Omega\,, \\ \mathrm{div}\,\boldsymbol{u} &= 0 \quad \text{in} \quad \Omega\,, \\ \boldsymbol{u} &= \boldsymbol{g} \quad \text{on} \quad \Gamma\,, \end{aligned} \tag{2.1}$$

where the unknowns are the velocity $\boldsymbol{u}$ and the pressure p of a non-Newtonian fluid occupying the region Ω. The flow is characterised by the nonlinear function $\mu : \mathbb{R}^+ \longrightarrow \mathbb{R}$ describing the viscosity field, a volume force $\boldsymbol{f} \in \mathbf{L}^2(\Omega)$, and the boundary velocity $\boldsymbol{g} \in \mathbf{H}^{1/2}(\Gamma)$ satisfying the compatibility condition $\int_\Gamma \boldsymbol{g}\cdot\boldsymbol{\nu} = 0$. Uniqueness of a pressure solution of (2.1) is ensured in the space

$$\mathrm{L}^2_0(\Omega) = \left\{ q \in L^2(\Omega) : \int_\Omega q = 0 \right\}.$$

Furthermore, we assume that μ is of class C^1, and that there exist constants μ_1, $\mu_2 > 0$, such that

$$\mu_1 \le \mu(s) \le \mu_2 \quad \text{and} \quad \mu_1 \le \mu(s) + s\,\mu'(s) \le \mu_2 \qquad \forall\, s \ge 0\,, \tag{2.2}$$

which imply Lipschitz-continuity and strong monotonicity of the nonlinear operator induced by μ, in the sense of the following result.

Lemma 2.1 *Let $L_\mu := \max\{\mu_2, 2\,\mu_2 - \mu_1\}$, where μ_1 and μ_2 are the bounds of μ given in (2.2). Then for each $\boldsymbol{r}$, $\boldsymbol{s} \in \mathbb{L}^2(\Omega)$ there holds*

$$\|\mu(|\boldsymbol{r}|)\,\boldsymbol{r} - \mu(|\boldsymbol{s}|)\,\boldsymbol{s}\|_{0,\Omega} \le L_\mu\,\|\boldsymbol{r}-\boldsymbol{s}\|_{0,\Omega}\,, \tag{2.3}$$

$$\int_\Omega \Big\{\mu(|\boldsymbol{r}|)\,\boldsymbol{r} - \mu(|\boldsymbol{s}|)\,\boldsymbol{s}\Big\} : \big(\boldsymbol{r}-\boldsymbol{s}\big) \ge \mu_1\,\|\boldsymbol{r}-\boldsymbol{s}\|^2_{0,\Omega}\,. \tag{2.4}$$

Proof. See [28, Theorem 3.8] for details. ∎

Typical examples of functions satisfying (2.2) are e.g. the classical power law and the Carreau parametrisation:

$$\mu(s) := 2 + (1+s)^{-1} \quad \text{and} \quad \mu(s) := \alpha_0 + \alpha_1(1+s^2)^{(\beta-2)/2}\,,$$

where α_0, $\alpha_1 > 0$ and $\beta \in [1,2]$.

Now, after introducing the additional tensor unknown, characterised by the constitutive law

$$\boldsymbol{\sigma} := \mu(|\nabla\boldsymbol{u}|)\,\nabla\boldsymbol{u} - (\boldsymbol{u}\otimes\boldsymbol{u}) - p\,\mathbb{I} \quad \text{in} \quad \Omega\,,$$

and applying the incompressibility constraint, we obtain

$$\mu(|\nabla \boldsymbol{u}|)\,\nabla \boldsymbol{u} \,-\, (\boldsymbol{u}\otimes\boldsymbol{u})^{\mathtt{d}} \,=\, \boldsymbol{\sigma}^{\mathtt{d}}, \quad p \,=\, -\frac{1}{n}\,\mathrm{tr}(\,\boldsymbol{\sigma}+\boldsymbol{u}\otimes\boldsymbol{u}\,) \quad \text{in} \quad \Omega\,, \tag{2.5}$$

which implies that the pressure can be eliminated from (2.1). Moreover, we also introduce the velocity gradient as an auxiliary variable $\boldsymbol{t} := \nabla \boldsymbol{u}$ in Ω. Consequently, we end up with the following system, expressed in terms of the unknowns $\boldsymbol{t}$, $\boldsymbol{\sigma}$, and $\boldsymbol{u}$:

$$\begin{aligned}
\nabla \boldsymbol{u} &= \boldsymbol{t} && \text{in} \quad \Omega\,,\\
\mu(|\boldsymbol{t}|)\,\boldsymbol{t} \,-\, (\boldsymbol{u}\otimes\boldsymbol{u})^{\mathtt{d}} &= \boldsymbol{\sigma}^{\mathtt{d}} && \text{in} \quad \Omega\,,\\
-\,\mathbf{div}\,\boldsymbol{\sigma} &= \boldsymbol{f} && \text{in} \quad \Omega\,,\\
\boldsymbol{u} &= \boldsymbol{g} && \text{on} \quad \Gamma\,,\\
\textstyle\int_\Omega \mathrm{tr}(\boldsymbol{\sigma} \,+\, \boldsymbol{u}\otimes\boldsymbol{u}) &= 0\,.
\end{aligned} \tag{2.6}$$

Notice from (2.5) that the required belonging of the pressure field to $\mathrm{L}^2_0(\Omega)$ is indeed guaranteed by the last equation of (2.6).

2.3 The augmented mixed formulation

Let us now recall that the augmented (through the incorporation of suitable Galerkin redundant terms) mixed formulation for (2.6), introduced in [11] and motivated by velocity regularity requirements, reads: Find $\vec{\boldsymbol{t}} := (\boldsymbol{t},\boldsymbol{\sigma},\boldsymbol{u}) \in \mathbf{H} := \mathbb{L}^2_{\mathtt{tr}}(\Omega)\times\mathbb{H}_0(\mathbf{div};\Omega)\times\mathbf{H}^1(\Omega)$ such that

$$\big[(\mathbf{A} \,+\, \mathbf{B}_{\boldsymbol{u}})(\vec{\boldsymbol{t}}),\vec{\boldsymbol{s}}\big] \,=\, \big[\mathbf{F},\vec{\boldsymbol{s}}\big] \qquad \forall\,\vec{\boldsymbol{s}} := (\boldsymbol{s},\boldsymbol{\tau},\boldsymbol{v}) \in \mathbf{H}\,, \tag{2.7}$$

where $\big[\cdot,\cdot\big]$ stands for the duality pairing between $\mathbf{H}'$ and $\mathbf{H}$, $\mathbf{A}:\mathbf{H}\longrightarrow\mathbf{H}'$ is the nonlinear operator

$$\begin{aligned}
\big[\mathbf{A}(\vec{\boldsymbol{t}}),\vec{\boldsymbol{s}}\big] \,:=\, &\int_\Omega \mu(|\boldsymbol{t}|)\,\boldsymbol{t}:\boldsymbol{s} \,-\, \int_\Omega \boldsymbol{\sigma}^{\mathtt{d}}:\boldsymbol{s} \,+\, \int_\Omega \boldsymbol{\tau}^{\mathtt{d}}:\boldsymbol{t} \,+\, \int_\Omega \boldsymbol{u}\cdot\mathbf{div}\,\boldsymbol{\tau} \,-\, \int_\Omega \boldsymbol{v}\cdot\mathbf{div}\,\boldsymbol{\sigma}\\
&+\, \kappa_1\int_\Omega \Big\{\boldsymbol{\sigma}^{\mathtt{d}} - \mu(|\boldsymbol{t}|)\,\boldsymbol{t}\Big\}:\boldsymbol{\tau}^{\mathtt{d}} \,+\, \kappa_2\int_\Omega \mathbf{div}\,\boldsymbol{\sigma}\cdot\mathbf{div}\,\boldsymbol{\tau}\\
&+\, \kappa_3\int_\Omega \Big\{\nabla\boldsymbol{u}-\boldsymbol{t}\Big\}:\nabla\boldsymbol{v} \,+\, \kappa_4\int_\Gamma \boldsymbol{u}\cdot\boldsymbol{v}\,,
\end{aligned}$$

the bounded linear functional $\mathbf{F}:\mathbf{H}\longrightarrow\mathrm{R}$ is defined as

$$\big[\mathbf{F},\vec{\boldsymbol{s}}\big] \,:=\, \langle\boldsymbol{\tau}\,\boldsymbol{\nu},\boldsymbol{g}\rangle \,+\, \int_\Omega \boldsymbol{f}\cdot\Big\{\boldsymbol{v} \,-\, \kappa_2\,\mathbf{div}\,\boldsymbol{\tau}\Big\} \,+\, \kappa_4\int_\Gamma \boldsymbol{g}\cdot\boldsymbol{v}\,,$$

where $\langle\cdot,\cdot\rangle$ denotes the duality pairing of $\mathbf{H}^{-1/2}(\Gamma)$ and $\mathbf{H}^{1/2}(\Gamma)$ with respect to the $\mathbf{L}^2(\Gamma)$-inner product, and for each $\boldsymbol{z}\in\mathbf{H}^1(\Omega)$, $\mathbf{B}_{\boldsymbol{z}}:\mathbf{H}\longrightarrow\mathbf{H}'$ is the bounded linear operator

$$\big[\mathbf{B}_{\boldsymbol{z}}(\vec{\boldsymbol{t}}),\vec{\boldsymbol{s}}\big] \,:=\, -\int_\Omega (\boldsymbol{z}\otimes\boldsymbol{u})^{\mathtt{d}}:\Big\{\kappa_1\,\boldsymbol{\tau}^{\mathtt{d}} \,+\, \boldsymbol{s}\Big\}\,,$$

for all $\vec{\boldsymbol{t}} := (\boldsymbol{t},\boldsymbol{\sigma},\boldsymbol{u})$, $\vec{\boldsymbol{s}} := (\boldsymbol{s},\boldsymbol{\tau},\boldsymbol{v}) \in \mathbf{H}$. The coefficients $\kappa_1,\kappa_2,\kappa_3,\kappa_4$ are positive parameters assuming the following values, dictated by the stability analysis of the augmented formulation: $\kappa_1 \in \left(0,\dfrac{2\delta\mu_1}{L_\mu}\right)$ and $\kappa_3 \in \left(0,2\widetilde{\delta}\left(\mu_1-\dfrac{\kappa_1\,L_\mu}{2\delta}\right)\right)$, with $\delta\in\left(0,\dfrac{2}{L_\mu}\right)$ and $\widetilde{\delta}\in(0,2)$, and $\kappa_2,\ \kappa_4>0$.

The unique solvability of (2.7) has been established in [11] using fixed point arguments. We omit details and refer the reader to [11, Sections 3.2 and 3.3]. Only for further use throughout the rest of the paper, we now let $\alpha(\Omega)$ be the strong monotonicity constant of the nonlinear operator $\mathbf{A}$ (cf. [11, eq. (3.23)]), and let $c_1(\Omega)$ and $c_{\mathbf{T}}$ be the boundedness constants specified in [11, eqs. (3.6), (3.19)]. In addition, we set (cf. [11, eq. (3.25)])

$$\rho_0 \,:=\, \frac{\alpha(\Omega)}{2\,c_1(\Omega)\,(\kappa_1^2+1)^{1/2}}\,. \tag{2.8}$$

2.4 The Galerkin scheme

Let us consider arbitrary finite dimensional subspaces $\mathbb{H}_h^{\boldsymbol{t}}$, $\mathbb{H}_h^{\boldsymbol{\sigma}}$ and $\mathbf{H}_h^{\boldsymbol{u}}$ of the continuous spaces $\mathbb{L}^2_{\mathtt{tr}}(\Omega)$, $\mathbb{H}_0(\mathbf{div};\Omega)$, and $\mathbf{H}^1(\Omega)$, respectively. As usual, h denotes the size of a regular triangulation $\mathcal{T}_h$ of $\overline{\Omega}$ made up of triangles K (when $n=2$) or tetrahedra K (when $n=3$) of diameter h_K, that is $h := \max\Big\{ h_K :\ K \in \mathcal{T}_h \Big\}$. Then, the Galerkin scheme associated with the nonlinear problem (2.7) reads: Find $\vec{\boldsymbol{t}}_h := (\boldsymbol{t}_h, \boldsymbol{\sigma}_h, \boldsymbol{u}_h) \in \mathbf{H}_h := \mathbb{H}_h^{\boldsymbol{t}} \times \mathbb{H}_h^{\boldsymbol{\sigma}} \times \mathbf{H}_h^{\boldsymbol{u}}$ such that

$$\big[\big(\mathbf{A} \,+\, \mathbf{B}_{\boldsymbol{u}_h}\big)(\vec{\boldsymbol{t}}_h), \vec{\boldsymbol{s}}_h\big] \,=\, \big[\mathbf{F}, \vec{\boldsymbol{s}}_h\big] \qquad \forall\, \vec{\boldsymbol{s}}_h \,:=\, (\boldsymbol{s}_h, \boldsymbol{\tau}_h, \boldsymbol{v}_h) \in \mathbf{H}_h\,. \tag{2.9}$$

Its linearised counterpart is defined via the discrete fixed point operator $\mathbf{T}_h : \mathbf{H}_h^{\boldsymbol{u}} \longrightarrow \mathbf{H}_h^{\boldsymbol{u}}$:

$$\mathbf{T}_h(\boldsymbol{z}_h) \,:=\, \boldsymbol{u}_h \qquad \forall\, \boldsymbol{z}_h \,\in\, \mathbf{H}_h^{\boldsymbol{u}}\,,$$

where $\boldsymbol{u}_h$ is the third component of the unique solution (to be confirmed by Theorem 2.2) of the discrete problem: Find $\vec{\boldsymbol{t}}_h := (\boldsymbol{t}_h, \boldsymbol{\sigma}_h, \boldsymbol{u}_h) \in \mathbf{H}_h$ such that

$$\big[\big(\mathbf{A} \,+\, \mathbf{B}_{\boldsymbol{z}_h}\big)(\vec{\boldsymbol{t}}_h), \vec{\boldsymbol{s}}_h\big] \,=\, \big[\mathbf{F}, \vec{\boldsymbol{s}}_h\big] \qquad \forall\, \vec{\boldsymbol{s}}_h \,:=\, \boldsymbol{s}_h, \boldsymbol{\tau}_h, \boldsymbol{v}_h) \in \mathbf{H}_h\,. \tag{2.10}$$

The well-posedness of the discrete problem is given in the following result

Theorem 2.2 *Given $\rho \in (0, \rho_0)$, with ρ_0 defined by (2.8), we let $W_\rho^h := \Big\{ \boldsymbol{z}_h \in \mathbf{H}_h^{\boldsymbol{u}} : \quad \|\boldsymbol{z}_h\|_{1,\Omega} \leq \rho \Big\}$, and assume that the data satisfy (cf. [11, eq. (3.27)])*

$$c_{\mathbf{T}} \Big\{ \|\boldsymbol{f}\|_{0,\Omega} \,+\, \|\boldsymbol{g}\|_{0,\Gamma} \,+\, \|\boldsymbol{g}\|_{1/2,\Gamma} \Big\} \,\leq\, \rho\,.$$

Then there exists a unique solution $\vec{\boldsymbol{t}}_h \in \mathbf{H}_h$ to (2.9) with $\boldsymbol{u}_h \in W_\rho^h$, and there holds

$$\|\vec{\boldsymbol{t}}_h\| \,\leq\, c_{\mathbf{T}} \Big\{ \|\boldsymbol{f}\|_{0,\Omega} \,+\, \|\boldsymbol{g}\|_{0,\Gamma} \,+\, \|\boldsymbol{g}\|_{1/2,\Gamma} \Big\}\,. \tag{2.11}$$

Proof. We refer the reader to [11, Lemma 4.1] for a detailed proof. ∎

In what follows, given an integer $k \geq 0$ and $T \in \mathcal{T}_h$, we let $\mathrm{P}_k(T)$ (resp. $\widetilde{\mathrm{P}}_k(T)$) be the space of polynomials on T of degree $\leq k$ (resp. of degree $= k$), and, as indicated at the beginning of Section 2.1, we set $\mathbf{P}_k(T) := [\mathrm{P}_k(T)]^n$ and $\mathbb{P}_k(T) := [\mathrm{P}_k(T)]^{n\times n}$. In turn, the global version of $\mathbf{P}_k(T)$ and $\mathbb{P}_k(T)$ are defined, respectively, as

$$\mathbf{P}_k(\mathcal{T}_h) := \Big\{ \boldsymbol{v}_h \in \mathbf{L}^2(\Omega) :\ \boldsymbol{v}_h\Big|_T \in \mathbf{P}_k(T) \quad \forall\, T \in \mathcal{T}_h \Big\}$$

and

$$\mathbb{P}_k(\mathcal{T}_h) := \Big\{ \boldsymbol{s}_h \in \mathbb{L}^2(\Omega) :\ \boldsymbol{s}_h\Big|_T \in \mathbb{P}_k(T) \quad \forall\, T \in \mathcal{T}_h \Big\}\,.$$

In addition, denoting by $\boldsymbol{x}$ a generic vector in R^n, we let $\mathbf{RT}_k(T)$ be the local Raviart–Thomas space of order k, that is

$$\mathbf{RT}_k(T) := \mathbf{P}_k(T) \,\oplus\, \widetilde{\mathrm{P}}_k(T)\,\boldsymbol{x}\,,$$

and define the tensor version of the corresponding global Raviart–Thomas space of order k as

$$\mathbb{RT}_k(\mathcal{T}_h) := \Big\{ \boldsymbol{\tau}_h \in \mathbb{H}(\mathbf{div};\Omega) : \ \boldsymbol{c}^t\,\boldsymbol{\tau}\Big|_T \in \mathbf{RT}_k(T) \quad \forall\, \boldsymbol{c} \in \mathrm{R}^n\,, \quad \forall\, T \in \mathcal{T}_h \Big\}\,.$$

Then, examples of specific finite element subspaces $\mathbb{H}_h^{\boldsymbol{t}}$, $\mathbb{H}_h^{\boldsymbol{\sigma}}$ and $\mathbf{H}_h^{\boldsymbol{u}}$ fulfilling Theorem 2.2 are approximations of $\boldsymbol{t}, \boldsymbol{\sigma}$ and $\boldsymbol{u}$ by piecewise polynomial tensors of degree $\leq k$, by tensor Raviart–Thomas elements of order k, and by continuous piecewise polynomial vectors of degree $\leq\ k+1$, respectively, that is

$$\begin{aligned} \mathbb{H}_h^{\boldsymbol{t}} &:= \mathbb{L}^2_{\mathtt{tr}}(\Omega) \cap \mathbb{P}_k(\mathcal{T}_h)\,, \\ \mathbb{H}_h^{\boldsymbol{\sigma}} &:= \mathbb{H}_0(\mathbf{div};\Omega) \cap \mathbb{RT}_k(\mathcal{T}_h)\,, \\ \mathbf{H}_h^{\boldsymbol{u}} &:= \Big\{ \boldsymbol{v}_h \in \mathbf{C}(\overline{\Omega}) : \ \boldsymbol{v}_h\Big|_T \in \mathbf{P}_{k+1}(T) \quad \forall\, T \in \mathcal{T}_h \Big\}\,. \end{aligned} \tag{2.12}$$

In such a framework, the following a priori error bounds are available (see the derivation in [11]):

Theorem 2.3 *Suppose that there exists $s > 0$ such that $\boldsymbol{t} \in \mathbb{H}^s(\Omega)$, $\boldsymbol{\sigma} \in \mathbb{H}^s(\Omega)$, $\mathbf{div}\,\boldsymbol{\sigma} \in \mathbf{H}^s(\Omega)$, and $\boldsymbol{u} \in \mathbf{H}^{s+1}(\Omega)$, and that the finite element subspaces are defined by* (2.12)*. Then, there exists $C > 0$, independent of h, such that for each $h > 0$ there holds*

$$\|\vec{\boldsymbol{t}} - \vec{\boldsymbol{t}}_h\| + \|p - p_h\|_{0,\Omega} \,\leq\, C\, h^{\min\{s,k+1\}} \Big\{ \|\boldsymbol{t}\|_{s,\Omega} \,+\, \|\boldsymbol{\sigma}\|_{s,\Omega} \,+\, \|\mathbf{div}\,\boldsymbol{\sigma}\|_{s,\Omega} \,+\, \|\boldsymbol{u}\|_{s+1,\Omega} \Big\}\,.$$

3 A posteriori error analysis: The 2D case

In this section we derive two reliable and efficient residual based a posteriori error estimators for the two-dimensional version of (2.10). The corresponding a posteriori error analysis for the 3D case, which follows from minor modifications of the one to be presented next, will be addressed in Section 4.

3.1 Preliminaries

Let $\mathcal{E}_h$ be the set of all edges of $\mathcal{T}_h$, and $\mathcal{E}(T)$ denotes the set of edges of a given $T \in \mathcal{T}_h$. Then $\mathcal{E}_h \,=\, \mathcal{E}_h(\Omega) \cup \mathcal{E}_h(\Gamma)$, where $\mathcal{E}_h(\Omega) := \{e \in \mathcal{E}_h : \quad e \subseteq \Omega\}$, $\mathcal{E}_h(\Gamma) := \{e \in \mathcal{E}_h : \quad e \subseteq \Gamma\}$. Moreover, h_e stands for the length of a given edge e. Also, for each edge $e \in \mathcal{E}_h$ we fix a unit normal vector $\boldsymbol{\nu}_e := (\nu_1, \nu_2)^{\mathtt{t}}$, and let $\boldsymbol{s}_e := (-\nu_2, \nu_1)^{\mathtt{t}}$ be the corresponding fixed unit tangential vector along e. However, when no confusion arises, we simple write $\boldsymbol{\nu}$ and $\boldsymbol{s}$ instead of $\boldsymbol{\nu}_e$ and $\boldsymbol{s}_e$, respectively. Now, let $\boldsymbol{v} \in \mathbf{L}^2(\Omega)$ such that $\boldsymbol{v}|_T \in \boldsymbol{C}(T)$ on each $T \in \mathcal{T}_h$. Then, given $T \in \mathcal{T}_h$ and $e \in \mathcal{E}(T) \cap \mathcal{E}_h(\Omega)$, we denote by $[\boldsymbol{v} \cdot \boldsymbol{s}]$ the tangential jump of $\boldsymbol{v}$ across e, that is $[\boldsymbol{v} \cdot \boldsymbol{s}] := (\boldsymbol{v}|_T - \boldsymbol{v}|_{T'})|_e \cdot \boldsymbol{s}$, where T and T' are the triangles of $\mathcal{T}_h$ having e as a common edge. Similar definitions hold for the tangential jumps of scalar and tensor fields $\varphi \in \mathrm{L}^2(\Omega)$ and $\boldsymbol{\tau} \in \mathbb{L}^2(\Omega)$, respectively, such that $\varphi|_T \in C(T)$ and $\boldsymbol{\tau}|_T \in \mathbb{C}(T)$ on each $T \in \mathcal{T}_h$.

Moreover, given scalar, vector, and tensor valued fields v, $\boldsymbol{\varphi} := (\varphi_1, \varphi_2)^{\mathtt{t}}$, and $\boldsymbol{\tau} =: (\tau_{ij})$, respectively, we denote

$$\mathbf{curl}\, v := \begin{pmatrix} \frac{\partial v}{\partial x_2} \\ -\frac{\partial v}{\partial x_1} \end{pmatrix}, \quad \underline{\mathbf{curl}}(\boldsymbol{\varphi}) := \begin{pmatrix} \mathbf{curl}(\varphi_1)^{\mathtt{t}} \\ \mathbf{curl}(\varphi_2)^{\mathtt{t}} \end{pmatrix} \quad \text{and} \quad \mathbf{curl}(\boldsymbol{\tau}) := \begin{pmatrix} \dfrac{\partial \tau_{12}}{\partial x_1} - \dfrac{\partial \tau_{11}}{\partial x_2} \\ \dfrac{\partial \tau_{22}}{\partial x_1} - \dfrac{\partial \tau_{21}}{\partial x_2} \end{pmatrix}.$$

Now, let $\mathbf{I}_h : \mathbf{H}^1(\Omega) \to \mathbf{X}_h$ be the vector version of the usual Clément interpolation operator (cf. [15]), where

$$\mathbf{X}_h := \left\{ \boldsymbol{\varphi}_h \in \mathbf{C}(\bar{\Omega}) : \quad \boldsymbol{\varphi}_h|_T \in \mathbf{P}_1(T) \quad \forall\, T \in \mathcal{T}_h \right\},$$

and let $\Pi_h : \mathbb{H}^1(\Omega) \to \mathbb{RT}_k(\mathcal{T}_h)$ be the Raviart-Thomas interpolator, which, according to its characterisation properties (see e.g. [22, Section 3.4.1]), verifies

$$\mathrm{div}(\Pi_h(\boldsymbol{\tau})) = \mathcal{P}_h(\mathrm{div}\,\boldsymbol{\tau}) \qquad \forall\, \boldsymbol{\tau} \in \mathbb{H}^1(\Omega)\,, \tag{3.1}$$

where $\mathcal{P}_h$ is the $\mathbf{L}^2(\Omega)$-orthogonal projector onto $\mathbf{P}_k(\mathcal{T}_h)$. Further approximation properties of $\mathbf{I}_h$ and Π_h are summarised in the following lemmas (see a proof in e.g. [15] and [22, Lemmas 3.16 and 3.18], respectively).

Lemma 3.1 *There exist c_1, $c_2 > 0$, independent of h, such that for all $\boldsymbol{\varphi} \in \mathbf{H}^1(\Omega)$ there holds*

$$\|\boldsymbol{\varphi} - \mathbf{I}_h(\boldsymbol{\varphi})\|_{0,T} \leq c_1\, h_T\, \|\boldsymbol{\varphi}\|_{1,\Delta(T)} \qquad \forall\, T \in \mathcal{T}_h\,,$$

and

$$\|\boldsymbol{\varphi} - \mathbf{I}_h(\boldsymbol{\varphi})\|_{0,e} \leq c_2\, h_e^{1/2}\, \|\boldsymbol{\varphi}\|_{1,\Delta(e)} \qquad \forall\, e \in \mathcal{E}_h(\Omega) \cup \mathcal{E}_h(\Gamma)\,,$$

where $\Delta(T) := \cup\{T' \in \mathcal{T}_h : \quad T' \cap T \neq \emptyset\}$ and $\Delta(e) := \cup\{T' \in \mathcal{T}_h : \quad T' \cap e \neq \emptyset\}$.

Lemma 3.2 *There exist C_1, $C_2 > 0$, independent of h, such that for all $\boldsymbol{\tau} \in \mathbb{H}^1(\Omega)$ there holds*

$$\|\boldsymbol{\tau} - \Pi_h(\boldsymbol{\tau})\|_{0,T} \leq C\, h_T\, \|\boldsymbol{\tau}\|_{1,T} \quad \forall\, T \in \mathcal{T}_h\,,$$

and

$$\|(\boldsymbol{\tau} - \Pi_h(\boldsymbol{\tau}))\,\boldsymbol{\nu}\|_{0,e} \leq C\, h_e^{1/2}\, \|\boldsymbol{\tau}\|_{1,T_e} \quad \forall\, e \in \mathcal{E}_h(\Omega) \cup \mathcal{E}_h(\Gamma)\,,$$

where T_e is a triangle of $\mathcal{T}_h$ containing the edge e on its boundary.

3.2 Error estimators and statement of our main results

Let $\vec{\boldsymbol{t}}_h := (\boldsymbol{t}_h, \boldsymbol{\sigma}_h, \boldsymbol{u}_h) \in \mathbf{H}_h$ be the unique solution of (2.10) and let us set the following residuals

$$\begin{aligned}
\boldsymbol{r}_1(\vec{\boldsymbol{t}}_h; \mathbf{0}) &:= \boldsymbol{\sigma}_h^{\mathtt{d}} - \mu(|\boldsymbol{t}_h|)\,\boldsymbol{t}_h + (\boldsymbol{u}_h \otimes \boldsymbol{u}_h)^{\mathtt{d}} \quad \text{in} \quad \Omega\,,\\
\boldsymbol{r}_2(\vec{\boldsymbol{t}}_h; \boldsymbol{f}) &:= \boldsymbol{f} + \mathbf{div}\,\boldsymbol{\sigma}_h \quad \text{in} \quad \Omega\,,\\
\boldsymbol{r}_3(\vec{\boldsymbol{t}}_h; \mathbf{0}) &:= \nabla \boldsymbol{u}_h - \boldsymbol{t}_h \quad \text{in} \quad \Omega\,,\\
\boldsymbol{r}_4(\vec{\boldsymbol{t}}_h; \boldsymbol{g}) &:= \boldsymbol{g} - \boldsymbol{u}_h \quad \text{on} \quad \Gamma\,.
\end{aligned} \tag{3.2}$$

Then, we define for each $T \in \mathcal{T}_h$ the (local) a posteriori error indicators

$$\theta_{1,T}^2 := \|\boldsymbol{r}_1(\vec{\boldsymbol{t}}_h; \mathbf{0})\|_{0,T}^2 + \|\boldsymbol{r}_2(\vec{\boldsymbol{t}}_h; \boldsymbol{f})\|_{0,T}^2 + \|\boldsymbol{r}_3(\vec{\boldsymbol{t}}_h; \mathbf{0})\|_{0,T}^2 + \sum_{e \in \mathcal{E}(T) \cap \mathcal{E}_h(\Gamma)} \|\boldsymbol{r}_4(\vec{\boldsymbol{t}}_h; \boldsymbol{g})\|_{0,e}^2\,, \tag{3.3}$$

and

$$\begin{aligned}
\theta_{2,T}^2 := \theta_{1,T}^2 &+ h_T^2 \|\mathbf{curl}(\boldsymbol{t}_h)\|_{0,T}^2 + \|\boldsymbol{f} - \mathcal{P}_h(\boldsymbol{f})\|_{0,T}^2\\
&+ \sum_{e \in \mathcal{E}(T) \cap \mathcal{E}_h(\Omega)} h_e \left\| \left[\boldsymbol{t}_h \boldsymbol{s}\right] \right\|_{0,e}^2 + \sum_{e \in \mathcal{E}(T) \cap \mathcal{E}_h(\Gamma)} h_e \left\| \frac{d\boldsymbol{g}}{d\boldsymbol{s}} - \boldsymbol{t}_h \boldsymbol{s} \right\|_{0,e}^2\,,
\end{aligned} \tag{3.4}$$

so that the global a posteriori error estimators are given, respectively, by

$$\boldsymbol{\theta}_1 \,:=\, \left\{ \sum_{T\in\mathcal{T}_h} \theta_{1,T}^2 \,+\, \|\boldsymbol{r}_4(\vec{\boldsymbol{t}}_h;\boldsymbol{g})\|_{1/2,\Gamma}^2 \right\}^{1/2} \quad \text{and} \quad \boldsymbol{\theta}_2 \,:=\, \left\{ \sum_{T\in\mathcal{T}_h} \theta_{2,T}^2 \right\}^{1/2} . \tag{3.5}$$

The main results of this section are as follows.

Theorem 3.3 *Assume that $\boldsymbol{f}\in\mathbf{L}^\infty(\Omega)$ and $\boldsymbol{g}\in\mathbf{H}^1(\Gamma)$, and that there holds (cf.* (2.8)*)*

$$c_{\mathbf{T}} \left\{ \|\boldsymbol{f}\| + \|\boldsymbol{g}\|_{0,\Gamma} + \|\boldsymbol{g}\|_{1/2,\Gamma} \right\} \leq \frac{\rho_0}{2} \,. \tag{3.6}$$

In addition, let $\vec{\boldsymbol{t}}\in\mathbf{H}$ and $\vec{\boldsymbol{t}}_h\in\mathbf{H}_h$ be the unique solutions of the continuous and discrete formulations (2.7) *and* (2.10)*, respectively. Then, there exist constants $C_{\mathtt{rel}}>0$ and $C_{\mathtt{eff}}>0$, independent of h, such that*

$$C_{\mathtt{eff}}\,\boldsymbol{\theta}_1 \,\leq\, \|\vec{\boldsymbol{t}}-\vec{\boldsymbol{t}}_h\| \,\leq\, C_{\mathtt{rel}}\,\boldsymbol{\theta}_1 \,. \tag{3.7}$$

Theorem 3.4 *Under the assumptions of Theorem 3.3, there exist constants $c_{\mathtt{rel}}>0$ and $c_{\mathtt{eff}}>0$, independent of h, such that*

$$c_{\mathtt{eff}}\,\boldsymbol{\theta}_2 \,\leq\, \|\vec{\boldsymbol{t}}-\vec{\boldsymbol{t}}_h\| \,\leq\, c_{\mathtt{rel}}\,\boldsymbol{\theta}_2 \,. \tag{3.8}$$

The upper and lower bounds in (3.7), (3.8) are known as the reliability and efficiency estimates, respectively, which are derived below in Sections 3.4 and 3.5 under the assumption that $\mathbf{f}$ and $\boldsymbol{g}$ are piecewise polynomials on $\mathcal{T}_h$ and the induced triangulation on Γ, respectively, for each $h>0$. Otherwise, higher order terms arising from polynomial approximations of these functions would appear in (3.7) and (3.8).

The analysis of the first a posteriori error estimator is straightforward, taking advantage of the fact that $\boldsymbol{u}\in\mathbf{H}^1(\Omega)$, which allows us to integrate by parts in some terms. For the second estimator, we exploit the properties of the Helmholtz decomposition jointly with the Clément and Raviart-Thomas interpolation operators. In this case, new terms that capture the jumps between triangles will appear.

3.3 A general a posteriori error estimate

In order to establish the reliability estimates of the a posteriori error estimators $\boldsymbol{\theta}_1$ and $\boldsymbol{\theta}_2$, that is the upper bounds in (3.7) and (3.8), and as announced in the Introduction, here we follow the strategy recently proposed in [21], which is based on the definition of a linear operator depending on the Gâteaux derivatives of the nonlinear terms of the formulation. More precisely, we begin with the following main result.

Lemma 3.5 *Assume that the data satisfy* (3.6)*, and let $\vec{\boldsymbol{t}}\in\mathbf{H}$ and $\vec{\boldsymbol{t}}_h\in\mathbf{H}_h$ be the unique solutions of the continuous and discrete formulations* (2.7) *and* (2.10)*, respectively. Then, there exists a constant $C>0$, independent of h, such that*

$$\|\vec{\boldsymbol{t}}-\vec{\boldsymbol{t}}_h\| \,\leq\, C \left\{ \|\mathbf{R}_1\|_{\mathbb{L}^2_{\mathrm{tr}}(\Omega)'} \,+\, \|\mathbf{R}_2\|_{\mathbb{H}_0(\mathbf{div};\Omega)'} \,+\, \|\mathbf{R}_3\|_{\mathbf{H}^1(\Omega)'} \right\}, \tag{3.9}$$

where $\mathbf{R}_1\in\mathbb{L}^2_{\mathrm{tr}}(\Omega)'$, $\mathbf{R}_2\in\mathbb{H}_0(\mathbf{div};\Omega)'$, and $\mathbf{R}_3\in\mathbf{H}^1(\Omega)'$, are defined by

$$\begin{aligned}
\mathbf{R}_1(\boldsymbol{s}) \;&:=\; \int_\Omega \boldsymbol{r}_1(\vec{\boldsymbol{t}}_h;\mathbf{0}) : \boldsymbol{s} \,, \\
\mathbf{R}_2(\boldsymbol{\tau}) \;&:=\; \langle \boldsymbol{\tau}\,\boldsymbol{\nu}, \boldsymbol{g}\rangle \,-\, \int_\Omega \boldsymbol{u}_h\cdot\mathbf{div}\,\boldsymbol{\tau} \,-\, \int_\Omega \boldsymbol{t}_h : \boldsymbol{\tau}^{\mathtt{d}} \\
&\quad -\,\kappa_1 \int_\Omega \boldsymbol{r}_1(\vec{\boldsymbol{t}}_h;\mathbf{0}) : \boldsymbol{\tau}^{\mathtt{d}} \,-\, \kappa_2 \int_\Omega \boldsymbol{r}_2(\vec{\boldsymbol{t}}_h;\boldsymbol{f})\cdot\mathbf{div}\,\boldsymbol{\tau} \,, \\
\mathbf{R}_3(\boldsymbol{v}) \;&:=\; \int_\Omega \boldsymbol{r}_2(\vec{\boldsymbol{t}}_h;\boldsymbol{f})\cdot\boldsymbol{v} \,-\, \kappa_3 \int_\Omega \boldsymbol{r}_3(\vec{\boldsymbol{t}}_h;\mathbf{0}) : \nabla\boldsymbol{v} \,+\, \kappa_4 \int_\Gamma \boldsymbol{r}_4(\vec{\boldsymbol{t}}_h;\boldsymbol{g})\cdot\boldsymbol{v} \,,
\end{aligned} \tag{3.10}$$

for all $\vec{\boldsymbol{s}} := (\boldsymbol{s},\boldsymbol{\tau},\boldsymbol{v}) \in \mathbf{H}$. *Furthermore, there holds*

$$\mathbf{R}_1(\boldsymbol{s}_h) + \mathbf{R}_2(\boldsymbol{\tau}_h) + \mathbf{R}_3(\boldsymbol{v}_h) = 0 \qquad \forall\, \vec{\boldsymbol{s}}_h := (\boldsymbol{s}_h,\boldsymbol{\tau}_h,\boldsymbol{v}_h) \in \mathbf{H}_h\,. \tag{3.11}$$

Proof. First of all, we recall from [11, proof of Lemma 3.4] that for each $\boldsymbol{z} \in \mathbf{H}^1(\Omega)$ such that $\|\boldsymbol{z}\|_{1,\Omega} \leq \rho_0$, $\mathbf{A} + \mathbf{B}_{\boldsymbol{z}}$ becomes strongly monotone with constant $\dfrac{\alpha(\Omega)}{2}$, that is

$$\big[\big(\mathbf{A} + \mathbf{B}_{\boldsymbol{z}}\big)(\vec{\boldsymbol{r}}) - \big(\mathbf{A} + \mathbf{B}_{\boldsymbol{z}}\big)(\vec{\boldsymbol{s}}), \vec{\boldsymbol{r}} - \vec{\boldsymbol{s}}\big] \geq \frac{\alpha(\Omega)}{2}\,\|\vec{\boldsymbol{r}} - \vec{\boldsymbol{s}}\|^2 \quad \forall\, \vec{\boldsymbol{r}} := (\boldsymbol{r},\boldsymbol{\zeta},\boldsymbol{w}),\ \vec{\boldsymbol{s}} := (\boldsymbol{s},\boldsymbol{\tau},\boldsymbol{v}) \in \mathbf{H}\,. \tag{3.12}$$

In addition, we note that $\mathbf{A}$ can be split in terms of a non-linear operator $\mathbf{A}_1 : \mathbb{L}^2_{\rm tr}(\Omega) \to \mathbb{L}^2_{\rm tr}(\Omega)'$, and a linear one $\mathbf{A}_2 : \mathbf{H} \to \mathbf{H}'$, namely

$$\big[\mathbf{A}(\vec{\boldsymbol{t}}), \vec{\boldsymbol{s}}\big] = = \big[\mathbf{A}_1(\boldsymbol{t}), \boldsymbol{s}\big] - \kappa_1\big[\mathbf{A}_1(\boldsymbol{t}), \boldsymbol{\tau}^d\big] + \big[\mathbf{A}_2\big(\vec{\boldsymbol{t}}\big), \vec{\boldsymbol{s}}\big]\,, \tag{3.13}$$

where

$$\big[\mathbf{A}_1(\boldsymbol{t}), \boldsymbol{s}\big] = \int_\Omega \mu(|\boldsymbol{t}|)\,\boldsymbol{t} : \boldsymbol{s}\,,$$

and

$$\begin{aligned}\big[\mathbf{A}_2\big(\vec{\boldsymbol{t}}\big), \vec{\boldsymbol{s}}\big] = &-\int_\Omega \boldsymbol{\sigma}^{\rm d} : \boldsymbol{s} + \int_\Omega \boldsymbol{\tau}^{\rm d} : \boldsymbol{t} + \int_\Omega \boldsymbol{u}\cdot\mathbf{div}\,\boldsymbol{\tau} - \int_\Omega \boldsymbol{v}\cdot\mathbf{div}\,\boldsymbol{\sigma} + \kappa_1\int_\Omega \boldsymbol{\sigma}^{\rm d} : \boldsymbol{\tau}^{\rm d} \\ &+ \kappa_2\int_\Omega \mathbf{div}\,\boldsymbol{\sigma}\cdot\mathbf{div}\,\boldsymbol{\tau} + \kappa_3\int_\Omega \Big\{\nabla\boldsymbol{u} - \boldsymbol{t}\Big\} : \nabla\boldsymbol{v} + \kappa_4\int_\Gamma \boldsymbol{u}\cdot\boldsymbol{v}\,,\end{aligned}$$

for all $\vec{\boldsymbol{t}} := (\boldsymbol{t},\boldsymbol{\sigma},\boldsymbol{u})$, $\vec{\boldsymbol{s}} := (\boldsymbol{s},\boldsymbol{\tau},\boldsymbol{v}) \in \mathbf{H}$. Note that hereafter $\big[\cdot,\cdot\big]$ stands for both the duality pairings between $\mathbf{H}'$ and $\mathbf{H}$ as before, and between $\mathbb{L}^2_{\rm tr}(\Omega)$ and $\mathbb{L}^2_{\rm tr}(\Omega)'$ as well. Next, we recall that the Gâteaux derivative of $\mathbf{A}_1$ maps $\mathbb{L}^2_{\rm tr}(\Omega)$ into $\mathcal{L}\big(\mathbb{L}^2_{\rm tr}(\Omega), \mathbb{L}^2_{\rm tr}(\Omega)'\big)$, so that, given $\boldsymbol{q} \in \mathbb{L}^2_{\rm tr}(\Omega)$, it is defined as

$$\mathcal{D}\mathbf{A}_1(\boldsymbol{q})(\boldsymbol{t})(\boldsymbol{s}) := \lim_{\varepsilon\to 0}\frac{\big[\mathbf{A}_1(\boldsymbol{q} + \varepsilon\,\boldsymbol{t}) - \mathbf{A}_1(\boldsymbol{q}), \boldsymbol{s}\big]}{\varepsilon} \qquad \forall\, \boldsymbol{t},\ \boldsymbol{s} \in \mathbb{L}^2_{\rm tr}(\Omega)\,.$$

It follows that $\mathcal{D}\mathbf{A}_1(\boldsymbol{q})$ can be considered as the bilinear form

$$\mathcal{D}\mathbf{A}_1(\boldsymbol{q})(\boldsymbol{t},\boldsymbol{s}) := \mathcal{D}\mathbf{A}_1(\boldsymbol{q})(\boldsymbol{t})(\boldsymbol{s}) \qquad \forall\, \boldsymbol{t},\ \boldsymbol{s} \in \mathbb{L}^2_{\rm tr}(\Omega)\,,$$

which, together with (3.13), suggests the introduction of the linear operator $\widetilde{\mathbf{A}}_{\boldsymbol{q}} : \mathbf{H} \to \mathbf{H}'$ (depending on the given $\boldsymbol{q}$), defined as

$$\big[\widetilde{\mathbf{A}}_{\boldsymbol{q}}(\vec{\boldsymbol{t}}), \vec{\boldsymbol{s}}\big] := \mathcal{D}\mathbf{A}_1(\boldsymbol{q})(\boldsymbol{t},\boldsymbol{s}) - \kappa_1\,\mathcal{D}\mathbf{A}_1(\boldsymbol{q})(\boldsymbol{t},\boldsymbol{\tau}^d) + \big[\mathbf{A}_2\big(\vec{\boldsymbol{t}}\big), \vec{\boldsymbol{s}}\big]\,, \tag{3.14}$$

for all $\vec{\boldsymbol{t}} := (\boldsymbol{t},\boldsymbol{\sigma},\boldsymbol{u})$, $\vec{\boldsymbol{s}} := (\boldsymbol{s},\boldsymbol{\tau},\boldsymbol{v}) \in \mathbf{H}$. Now, it is easy to see that the properties (2.3) and (2.4) satisfied by μ (cf. Lemma 2.1) imply that $\mathcal{D}\mathbf{A}_1(\boldsymbol{q})(\cdot,\cdot)$ is uniformly bounded and uniformly elliptic with constants L_μ and μ_1, respectively, and hence, proceeding similarly as for the derivation of (3.12), we find that, given $\boldsymbol{z} \in \mathbf{H}^1(\Omega)$ such that $\|\boldsymbol{z}\|_{1,\Omega} \leq \rho_0$, the bilinear form $\widetilde{\mathbf{A}}_{\boldsymbol{q}} + \mathbf{B}_{\boldsymbol{z}}$ becomes uniformly elliptic with the same constant $\dfrac{\alpha(\Omega)}{2}$ from (3.12), that is

$$[(\widetilde{\mathbf{A}}_{\boldsymbol{q}} + \mathbf{B}_{\boldsymbol{z}})(\vec{\boldsymbol{r}}), \vec{\boldsymbol{r}}] \geq \frac{\alpha(\Omega)}{2}\|\vec{\boldsymbol{r}}\|^2 \qquad \forall\, \vec{\boldsymbol{r}} \in \mathbf{H}\,,$$

which, in turn, implies the inf-sup condition

$$\frac{\alpha(\Omega)}{2}\|\vec{\boldsymbol{r}}\| \,\leq\, \sup_{\substack{\vec{\boldsymbol{s}}\in\mathbb{H}\\ \vec{\boldsymbol{s}}\neq\mathbf{0}}} \frac{[(\widetilde{\mathbf{A}}_{\boldsymbol{q}}+\mathbf{B}_{\boldsymbol{z}})(\vec{\boldsymbol{r}}),\vec{\boldsymbol{s}}]}{\|\vec{\boldsymbol{s}}\|} \qquad \forall\,\vec{\boldsymbol{r}}\in\mathbf{H}\,. \tag{3.15}$$

On the other hand, using the Mean Value Theorem, we can assert that there exists a convex combination $\boldsymbol{q}_h$ between $\boldsymbol{t}$ and $\boldsymbol{t}_h$ such that

$$\mathcal{D}\mathbf{A}_1(\boldsymbol{q}_h)(\boldsymbol{t}-\boldsymbol{t}_h,\boldsymbol{s}) = [\mathbf{A}_1(\boldsymbol{t}),\boldsymbol{s}] - [\mathbf{A}_1(\boldsymbol{t}_h),\boldsymbol{s}] \qquad \forall\,\boldsymbol{s}\,\in\,\mathbb{L}^2_{\rm tr}(\Omega)\,. \tag{3.16}$$

In this way, applying (3.15) to $\vec{\boldsymbol{r}} = \vec{\boldsymbol{t}}-\vec{\boldsymbol{t}}_h$, with $\boldsymbol{q}=\boldsymbol{q}_h$ and $\boldsymbol{z}=\boldsymbol{u}$, where $\boldsymbol{u}$ is the third component of the exact solution $\vec{\boldsymbol{t}}\in\mathbf{H}$, we can write

$$\frac{\alpha(\Omega)}{2}\|\vec{\boldsymbol{t}}-\vec{\boldsymbol{t}}_h\| \leq \sup_{\substack{\vec{\boldsymbol{s}}\in\mathbb{H}\\ \vec{\boldsymbol{s}}\neq\mathbf{0}}} \frac{[(\widetilde{\mathbf{A}}_{\boldsymbol{q}_h}+\mathbf{B}_{\boldsymbol{u}})(\vec{\boldsymbol{t}}-\vec{\boldsymbol{t}}_h),\vec{\boldsymbol{s}}]}{\|\vec{\boldsymbol{s}}\|}\,, \tag{3.17}$$

where, thanks to (3.14), (3.16), (2.7), and minor algebraic manipulations, we find that

$$\begin{aligned}[(\widetilde{\mathbf{A}}_{\boldsymbol{q}_h}+\mathbf{B}_{\boldsymbol{u}})(\vec{\boldsymbol{t}}-\vec{\boldsymbol{t}}_h),\vec{\boldsymbol{s}}] \,&=\, [\mathbf{F},\vec{\boldsymbol{s}}] \,-\, [(\mathbf{A}\,+\,\mathbf{B}_{\boldsymbol{u}})(\vec{\boldsymbol{t}}_h),\vec{\boldsymbol{s}}]\\ &=\quad [\mathbf{F},\vec{\boldsymbol{s}}] \,-\, [(\mathbf{A}\,+\,\mathbf{B}_{\boldsymbol{u}_h})(\vec{\boldsymbol{t}}_h),\vec{\boldsymbol{s}}] \,+\, [\mathbf{B}_{\boldsymbol{u}_h-\boldsymbol{u}}(\vec{\boldsymbol{t}}_h),\vec{\boldsymbol{s}}]\,.\end{aligned} \tag{3.18}$$

Next, we recall from [11, eq. (3.21)] that

$$\big|\,[\mathbf{B}_{\boldsymbol{u}_h-\boldsymbol{u}}(\vec{\boldsymbol{t}}_h),\vec{\boldsymbol{s}}]\,\big| \,\leq\, c_1(\Omega)\,(\kappa_1^2+1)^{1/2}\,\|\boldsymbol{u}_h-\boldsymbol{u}\|_{1,\Omega}\,\|\vec{\boldsymbol{t}}_h\|\,\|\vec{\boldsymbol{s}}\|\,,$$

which, employing (2.8), the a priori estimate (2.11), the assumption (3.6), and the fact that obviously $\|\boldsymbol{u}_h-\boldsymbol{u}\|_{1,\Omega}\,\leq\,\|\vec{\boldsymbol{t}}-\vec{\boldsymbol{t}}_h\|$, yields

$$\big|\,[\mathbf{B}_{\boldsymbol{u}_h-\boldsymbol{u}}(\vec{\boldsymbol{t}}_h),\vec{\boldsymbol{s}}]\,\big| \,\leq\, \frac{\alpha(\Omega)}{4}\,\|\vec{\boldsymbol{t}}-\vec{\boldsymbol{t}}_h\|\,\|\vec{\boldsymbol{s}}\|\,. \tag{3.19}$$

Thus, replacing (3.18) back into (3.17), and then using (3.19), we arrive at

$$\frac{\alpha(\Omega)}{4}\|\vec{\boldsymbol{t}}-\vec{\boldsymbol{t}}_h\| \leq \sup_{\substack{\vec{\boldsymbol{s}}\in\mathbb{H}\\ \vec{\boldsymbol{s}}\neq\mathbf{0}}} \frac{\big|[\mathbf{F},\vec{\boldsymbol{s}}] \,-\, [(\mathbf{A}\,+\,\mathbf{B}_{\boldsymbol{u}_h})(\vec{\boldsymbol{t}}_h),\vec{\boldsymbol{s}}]\big|}{\|\vec{\boldsymbol{s}}\|}\,,$$

from which (3.9) is obtained by observing that

$$[\mathbf{F},\vec{\boldsymbol{s}}] \,-\, [(\mathbf{A}\,+\,\mathbf{B}_{\boldsymbol{u}_h})(\vec{\boldsymbol{t}}_h),\vec{\boldsymbol{s}}] \,=\, \mathbf{R}_1(\boldsymbol{s}) \,+\, \mathbf{R}_2(\boldsymbol{\tau}) \,+\, \mathbf{R}_3(\boldsymbol{v}) \qquad \forall\,\vec{\boldsymbol{s}} \,:=\, (\boldsymbol{s},\boldsymbol{\tau},\boldsymbol{v})\in\mathbf{H}\,.$$

Finally, it is readily seen that (3.11) follows directly from (2.9) and the foregoing identity. ∎

We end this section with an alternative expression for the functional $\mathbf{R}_2$. In fact, noting that

$$\int_\Omega \boldsymbol{t}_h:\boldsymbol{\tau}^{\mathtt{d}} = \int_\Omega \boldsymbol{t}_h^{\mathtt{d}}:\boldsymbol{\tau} = \int_\Omega \boldsymbol{t}_h:\boldsymbol{\tau} \tag{3.20}$$

and

$$\int_\Omega \boldsymbol{r}_1(\vec{\boldsymbol{t}}_h;\mathbf{0}):\boldsymbol{\tau}^{\mathtt{d}} = \int_\Omega \boldsymbol{r}_1(\vec{\boldsymbol{t}}_h;\mathbf{0})^{\mathtt{d}}:\boldsymbol{\tau} = \int_\Omega \boldsymbol{r}_1(\vec{\boldsymbol{t}}_h;\mathbf{0}):\boldsymbol{\tau}\,, \tag{3.21}$$

and then integrating by parts the expression $\displaystyle\int_\Omega \boldsymbol{u}_h\cdot\mathbf{div}\,\boldsymbol{\tau}$, we find that $\mathbf{R}_2(\boldsymbol{\tau})$ can be rewritten as

$$\mathbf{R}_2(\boldsymbol{\tau}) \,=\, -\,\kappa_1\,\int_\Omega \boldsymbol{r}_1(\vec{\boldsymbol{t}}_h;\mathbf{0}):\boldsymbol{\tau} - \,\kappa_2\,\int_\Omega \boldsymbol{r}_2(\vec{\boldsymbol{t}}_h;\boldsymbol{f})\cdot\mathbf{div}\,\boldsymbol{\tau} \,+\, \int_\Omega \boldsymbol{r}_3(\vec{\boldsymbol{t}}_h;\mathbf{0}):\boldsymbol{\tau} \,+\, \big\langle\boldsymbol{\tau}\,\boldsymbol{\nu},\boldsymbol{r}_4(\vec{\boldsymbol{t}}_h;\boldsymbol{g})\big\rangle\,. \tag{3.22}$$

3.4 Reliability of the a posteriori error estimators

We now proceed to bound the norms appearing on the right hand side of (3.9) of the functionals $\mathbf{R}_i$, $i \in \{1,2,3\}$, defined in (3.10). This task is performed in two different ways, which leads to the reliability of the a posteriori error estimators $\boldsymbol{\theta}_1$ and $\boldsymbol{\theta}_2$. We begin with $\boldsymbol{\theta}_1$.

Theorem 3.6 *Assume that the data satisfy* (3.6)*, and let* $\vec{\boldsymbol{t}} \in \mathbf{H}$ *and* $\vec{\boldsymbol{t}}_h \in \mathbf{H}_h$ *be the unique solutions of the continuous and discrete formulations* (2.7) *and* (2.10)*, respectively. Then there exists* $C_{\mathtt{rel}} > 0$*, independent of* h*, such that*

$$\|\vec{\boldsymbol{t}} - \vec{\boldsymbol{t}}_h\| \, \leq \, C_{\mathtt{rel}} \, \boldsymbol{\theta}_1 \, . \tag{3.23}$$

Proof. We first observe from (3.10) that simple applications of the Cauchy-Schwarz inequality yield

$$\|\mathbf{R}_1\|_{\mathbb{L}^2_{\mathrm{tr}}(\Omega)'} \, \leq \, \|\boldsymbol{r}_1(\vec{\boldsymbol{t}}_h;\mathbf{0})\|_{0,\Omega} \tag{3.24}$$

and

$$\|\mathbf{R}_3\|_{\mathbf{H}^1(\Omega)'} \, \leq \, c_3 \Big\{ \|\boldsymbol{r}_2(\vec{\boldsymbol{t}}_h;\boldsymbol{f})\|_{0,\Omega} \, + \, \|\boldsymbol{r}_3(\vec{\boldsymbol{t}}_h;\mathbf{0})\|_{0,\Omega} \, + \, \|\boldsymbol{r}_4(\vec{\boldsymbol{t}}_h;\boldsymbol{g})\|_{0,\Gamma} \Big\} \, , \tag{3.25}$$

where $c_3 > 0$ is a constant depending on κ_3, κ_4, and the norm of the trace operator mapping $\mathbf{H}^1(\Omega)$ into $\mathbf{L}^2(\Gamma)$. In turn, employing again the Cauchy-Schwarz inequality, and recalling that $\langle \cdot , \cdot \rangle$ stands for the duality pairing between $\mathbf{H}^{-1/2}(\Gamma)$ and $\mathbf{H}^{1/2}(\Gamma)$, we deduce from (3.22) that

$$\|\mathbf{R}_2\|_{\mathbb{H}_0(\mathbf{div};\Omega)'} \, \leq \, c_2 \Big\{ \|\boldsymbol{r}_1(\vec{\boldsymbol{t}}_h;\mathbf{0})\|_{0,\Omega} \, + \, \|\boldsymbol{r}_2(\vec{\boldsymbol{t}}_h;\boldsymbol{f})\|_{0,\Omega} \, + \, \|\boldsymbol{r}_3(\vec{\boldsymbol{t}}_h;\mathbf{0})\|_{0,\Omega} \, + \, \|\boldsymbol{r}_4(\vec{\boldsymbol{t}}_h;\boldsymbol{g})\|_{1/2,\Gamma} \Big\} \, , \tag{3.26}$$

where $c_2 > 0$ is a constant depending on κ_1, κ_2, and the norm of the trace operator mapping $\mathbf{H}^1(\Omega)$ onto $\mathbf{H}^{1/2}(\Gamma)$. In this way, replacing the bounds (3.24), (3.25), and (3.26) back into (3.9) we arrive at the required inequality (3.23) with $\boldsymbol{\theta}_1$ given in (3.5). ∎

Having proved Theorem 3.6, we now aim to establish the reliability of $\boldsymbol{\theta}_2$ (cf. (3.5)). To this end, we first remark that the estimation of $\|\mathbf{R}_1\|_{\mathbb{L}^2_{\mathrm{tr}}(\Omega)'}$ and $\|\mathbf{R}_3\|_{\mathbf{H}^1(\Omega)'}$ is performed exactly as in (3.24) and (3.25), and that the new a posteriori error estimator $\boldsymbol{\theta}_2$ arises from a different way of bounding $\|\mathbf{R}_2\|_{\mathbb{H}_0(\mathbf{div};\Omega)'}$. More precisely, we derive this estimate by focusing on the terms arising after exploiting the Helmholtz decomposition provided by the following lemma.

Lemma 3.7 *For each* $\boldsymbol{\tau} \in \mathbb{H}_0(\mathbf{div};\Omega)$ *there exist* $\boldsymbol{z} \in \mathbf{H}^2(\Omega)$ *and* $\boldsymbol{\varphi} \in \mathbf{H}^1(\Omega)$ *such that*

$$\boldsymbol{\tau} \, = \, \nabla \boldsymbol{z} \, + \, \underline{\mathbf{curl}}(\boldsymbol{\varphi}) \quad \textit{in} \quad \Omega \quad \textit{and} \quad \|\boldsymbol{z}\|_{2,\Omega} \, + \, \|\boldsymbol{\varphi}\|_{1,\Omega} \, \leq \, c \, \|\boldsymbol{\tau}\|_{\mathbf{div};\Omega} \, , \tag{3.27}$$

where c *is a positive constant independent of all the foregoing variables.*

Proof. The proof proceeds exactly as in [26, Section 4] (see also [17, Lemma 3.4]). We provide details in what follows just for sake of completeness. We begin by introducing a bounded convex polygonal domain G containing $\bar{\Omega}$. Then, given $\boldsymbol{\tau} \in \mathbb{H}_0(\mathbf{div};\Omega)$, we define $\boldsymbol{z} := \boldsymbol{w}|_\Omega$, where $\boldsymbol{w} \in \mathbf{H}^1(G)$ is the unique weak solution of the boundary value problem:

$$\Delta \boldsymbol{w} \, = \, \begin{cases} \mathbf{div}\, \boldsymbol{\tau} & \text{in } \Omega \\ \mathbf{0} & \text{in } G \backslash \Omega \end{cases} \, , \quad \boldsymbol{w} \, = \, \mathbf{0} \quad \text{on } \partial G \, . \tag{3.28}$$

The elliptic regularity result for (3.28) establishes that $\boldsymbol{w} \in \mathbf{H}^2(G)$, which certainly implies $\boldsymbol{z} \in \mathbf{H}^2(\Omega)$, and there holds

$$\|\boldsymbol{z}\|_{2,\Omega} \, \leq \, \|\boldsymbol{w}\|_{2,G} \, \leq \, \|\mathbf{div}\, \boldsymbol{\tau}\|_{0,\Omega} \, . \tag{3.29}$$

Next, since $\mathbf{div}(\boldsymbol{\tau}-\nabla\boldsymbol{z}) = 0 \quad \text{in} \quad \Omega$, and Ω is connected, an already classical result (cf. [29, Chapter I, Theorem 3.1]) guarantees the existence of $\boldsymbol{\varphi} = (\varphi_1,\varphi_2)^{\mathtt{t}} \in \mathbf{H}^1(\Omega)$, which can be chosen so that $\displaystyle\int_\Omega \varphi_1 = \int_\Omega \varphi_2 = 0$, such that

$$\boldsymbol{\tau} - \nabla\boldsymbol{z} = \underline{\mathbf{curl}}(\boldsymbol{\varphi}) \quad \text{in} \quad \Omega\,, \tag{3.30}$$

which proves the identity in (3.27). In turn, the equivalence between $\|\boldsymbol{\varphi}\|_{1,\Omega}$ and $|\boldsymbol{\varphi}|_{1,\Omega}$ (which is consequence of the generalised Poincaré inequality), together with (3.29) and (3.30), imply

$$\|\boldsymbol{\varphi}\|_{1,\Omega} \leq C\,|\boldsymbol{\varphi}|_{1,\Omega} = C\,\|\underline{\mathbf{curl}}(\boldsymbol{\varphi})\|_{0,\Omega} \leq C\left\{\|\boldsymbol{\tau}\|_{0,\Omega} + |\boldsymbol{z}|_{1,\Omega}\right\} \leq C\,\|\boldsymbol{\tau}\|_{\mathrm{div},\Omega}\,.$$

Finally, the foregoing inequality and (3.29) confirm the stability estimate on the right hand side of (3.27), thus finishing the proof.

∎

We now introduce a discrete version of the identity in (3.27). In fact, given again $\boldsymbol{\tau} \in \mathbb{H}_0(\mathbf{div};\Omega)$ with $\boldsymbol{z}$ and $\boldsymbol{\varphi}$ satisfying (3.27), and recalling from Section 3.1 that $\mathbf{I}_h$ and Π_h denote the Clément and Raviart-Thomas interpolators, respectively, we let $\boldsymbol{\varphi}_h := \mathbf{I}_h(\boldsymbol{\varphi})$ and set

$$\widetilde{\boldsymbol{\tau}}_h := \Pi_h(\nabla\boldsymbol{z}) + \underline{\mathbf{curl}}(\boldsymbol{\varphi}_h) + c_h\,\mathbb{I}\,, \tag{3.31}$$

where $c_h \in \mathrm{R}$ is chosen so that $\widetilde{\boldsymbol{\tau}}_h$, which is already in $\mathbb{RT}_k(\mathcal{T}_h)$, belongs to $\mathbb{H}_h^{\boldsymbol{\sigma}}$ (cf. (2.12)). Equivalently, $\widetilde{\boldsymbol{\tau}}_h$ is the $\mathbb{H}_0(\mathbf{div};\Omega)$-component of $\underline{\mathbf{curl}}(\boldsymbol{\varphi}_h) + \Pi_h(\nabla\boldsymbol{z}) \in \mathbb{RT}_k(\mathcal{T}_h)$. We refer to (3.31) as a discrete Helmholtz decomposition of $\boldsymbol{\tau}$.

According to the above, and employing from (3.11) that $\mathbf{R}_2(\widetilde{\boldsymbol{\tau}}_h) = 0$, we deduce thanks to the linearity of $\mathbf{R}_2$ and the fact that $\mathbf{R}_2(\mathbb{I}) = 0$ (which follows from (3.10) and the compatibility condition for the Dirichlet datum $\boldsymbol{g}$ explained in Section 2.1), that the expression $\mathbf{R}_2(\boldsymbol{\tau})$ can be decomposed as

$$\mathbf{R}_2(\boldsymbol{\tau}) = \mathbf{R}_2(\boldsymbol{\tau}-\widetilde{\boldsymbol{\tau}}_h) = \mathbf{R}_2\big(\nabla\boldsymbol{z} - \Pi_h(\nabla\boldsymbol{z})\big) + \mathbf{R}_2\big(\underline{\mathbf{curl}}(\boldsymbol{\varphi}-\boldsymbol{\varphi}_h)\big)\,. \tag{3.32}$$

Consequently, in what follows we derive suitable upper bounds for the modules of the two expressions on the right hand side of the foregoing equation. To this end, we now recall from [17] the following integration by parts formula on the boundary.

Lemma 3.8 *There holds*

$$\langle\underline{\mathbf{curl}}\,\psi\,\boldsymbol{\nu},\boldsymbol{\chi}\rangle = -\langle\frac{d\boldsymbol{\chi}}{d\mathbf{s}},\psi\rangle \qquad \forall\,\psi,\,\boldsymbol{\chi} \in \mathbf{H}^1(\Omega)\,. \tag{3.33}$$

Proof. The proof follows from suitable applications of the Green formulae provided in [29, Chapter I, eq. (2.17) and Theorem 2.11]. For details, we refer to [17, Lemma 3.5, eq. (3.35)]

∎

The estimate for $\big|\,\mathbf{R}_2\big(\underline{\mathbf{curl}}(\boldsymbol{\varphi}-\boldsymbol{\varphi}_h)\big)\,\big|$ is given first.

Lemma 3.9 *Assume that $\boldsymbol{g} \in \mathbf{H}^1(\Gamma)$. Then there exists $C>0$, independent of h, such that*

$$\big|\,\mathbf{R}_2\big(\underline{\mathbf{curl}}(\boldsymbol{\varphi}-\boldsymbol{\varphi}_h)\big)\,\big| \leq C\left\{\sum_{T\in\mathcal{T}_h}\widetilde{\theta}^2_{2,T}\right\}^{1/2}\|\boldsymbol{\varphi}\|_{1,\Omega}\,, \tag{3.34}$$

where

$$\widetilde{\theta}^2_{2,T} := h_T^2 \|\mathbf{curl}(\boldsymbol{t}_h)\|^2_{0,T} + \sum_{e \in \mathcal{E}(T)\cap\mathcal{E}_h(\Omega)} h_e \, \|[\boldsymbol{t}_h \, \boldsymbol{s}]\|^2_{0,e}$$
$$+ \sum_{e \in \mathcal{E}(T)\cap\mathcal{E}_h(\Gamma)} h_e \left\| \frac{d\boldsymbol{g}}{d\boldsymbol{s}} - \boldsymbol{t}_h \boldsymbol{s} \right\|^2_{0,e} + \|\boldsymbol{r}_1(\vec{\boldsymbol{t}}_h; \mathbf{0})\|^2_{0,T} \, .$$

Proof. We begin by observing from the definition of the functional $\mathbf{R}_2$ (cf. (3.10)) and the identities (3.20) and (3.21) that

$$\begin{aligned} \mathbf{R}_2\big(\underline{\mathbf{curl}}(\boldsymbol{\varphi} - \boldsymbol{\varphi}_h)\big) \, = \, \langle \underline{\mathbf{curl}}(\boldsymbol{\varphi} - \boldsymbol{\varphi}_h) \, \boldsymbol{\nu}, \boldsymbol{g} \rangle \, - \, \int_\Omega \boldsymbol{t}_h : \underline{\mathbf{curl}}(\boldsymbol{\varphi} - \boldsymbol{\varphi}_h) \\ - \, \kappa_1 \int_\Omega \boldsymbol{r}_1(\vec{\boldsymbol{t}}_h; \mathbf{0}) : \underline{\mathbf{curl}}(\boldsymbol{\varphi} - \boldsymbol{\varphi}_h) \, . \end{aligned} \tag{3.35}$$

Note that, alternatively, we could have employed the expression (3.22) for $\mathbf{R}_2$. Then, applying (3.33) (cf. Lemma 3.8) to $\boldsymbol{\psi} = \boldsymbol{\varphi} - \boldsymbol{\varphi}_h$ and to a trace lifting $\boldsymbol{\chi}$ of $\boldsymbol{g}$, and then using from the hypothesis that $\dfrac{d\boldsymbol{g}}{d\mathbf{s}} \in \mathbf{L}^2(\Gamma)$, we find that

$$\langle \underline{\mathbf{curl}}(\boldsymbol{\varphi} - \boldsymbol{\varphi}_h) \, \boldsymbol{\nu}, \boldsymbol{g} \rangle \, = \, - \Big\langle \frac{d\boldsymbol{g}}{d\mathbf{s}}, \boldsymbol{\varphi} - \boldsymbol{\varphi}_h \Big\rangle \, = \, - \sum_{e \in \mathcal{E}_h(\Gamma)} \int_e (\boldsymbol{\varphi} - \boldsymbol{\varphi}_h) \, \frac{d\boldsymbol{g}}{d\mathbf{s}} \, . \tag{3.36}$$

In turn, integrating by parts on each $T \in \mathcal{T}_h$, we obtain that

$$\begin{aligned} \int_\Omega \boldsymbol{t}_h : \underline{\mathbf{curl}}(\boldsymbol{\varphi} - \boldsymbol{\varphi}_h) \, = \, \sum_{T \in \mathcal{T}_h} \int_T \boldsymbol{t}_h : \underline{\mathbf{curl}}(\boldsymbol{\varphi} - \boldsymbol{\varphi}_h) \, = \, \sum_{T \in \mathcal{T}_h} \int_T \mathbf{curl}(\boldsymbol{t}_h) \cdot (\boldsymbol{\varphi} - \boldsymbol{\varphi}_h) \\ - \sum_{e \in \mathcal{E}_h(\Omega)} \int_e [\boldsymbol{t}_h \boldsymbol{s}] \cdot (\boldsymbol{\varphi} - \boldsymbol{\varphi}_h) \, - \, \sum_{e \in \mathcal{E}_h(\Gamma)} \int_e \boldsymbol{t}_h \boldsymbol{s} \cdot (\boldsymbol{\varphi} - \boldsymbol{\varphi}_h) \, , \end{aligned}$$

which, together with (3.36), yields

$$\begin{aligned} \langle \underline{\mathbf{curl}}(\boldsymbol{\varphi} - \boldsymbol{\varphi}_h) \, \boldsymbol{\nu}, \boldsymbol{g} \rangle \, - \, \int_\Omega \boldsymbol{t}_h : \underline{\mathbf{curl}}(\boldsymbol{\varphi} - \boldsymbol{\varphi}_h) \, = \, - \sum_{T \in \mathcal{T}_h} \int_T \mathbf{curl}(\boldsymbol{t}_h) \cdot (\boldsymbol{\varphi} - \boldsymbol{\varphi}_h) \\ + \sum_{e \in \mathcal{E}_h(\Omega)} \int_e [\boldsymbol{t}_h \boldsymbol{s}] \cdot (\boldsymbol{\varphi} - \boldsymbol{\varphi}_h) \, - \, \sum_{e \in \mathcal{E}_h(\Gamma)} \int_e \left\{ \frac{d\boldsymbol{g}}{d\mathbf{s}} - \boldsymbol{t}_h \boldsymbol{s} \right\} \cdot (\boldsymbol{\varphi} - \boldsymbol{\varphi}_h) \end{aligned} \tag{3.37}$$

In this way, applying the Cauchy-Schwarz inequality, the approximation properties of the Clément interpolator $\mathbf{I}_h$ (cf. Lemma 3.1), and the fact that the number of triangles of the macro-elements $\Delta(T)$ and $\Delta(e)$ are uniformly bounded, we deduce from (3.37) that

$$\left| \langle \underline{\mathbf{curl}}(\boldsymbol{\varphi} - \boldsymbol{\varphi}_h) \, \boldsymbol{\nu}, \boldsymbol{g} \rangle \, - \, \int_\Omega \boldsymbol{t}_h : \underline{\mathbf{curl}}(\boldsymbol{\varphi} - \boldsymbol{\varphi}_h) \right| \, \leq \, C \left\{ \sum_{T \in \mathcal{T}_h} \overline{\theta}^2_{2,T} \right\}^{1/2} \|\boldsymbol{\varphi}\|_{1,\Omega} \, , \tag{3.38}$$

where $C > 0$ is independent of h, and

$$\overline{\theta}^2_{2,T} := h_T^2 \|\mathbf{curl}(\boldsymbol{t}_h)\|^2_{0,T} + \sum_{e \in \mathcal{E}(T)\cap\mathcal{E}_h(\Omega)} h_e \, \|[\boldsymbol{t}_h \, \boldsymbol{s}]\|^2_{0,e} + \sum_{e \in \mathcal{E}(T)\cap\mathcal{E}_h(\Gamma)} h_e \left\| \frac{d\boldsymbol{g}}{d\boldsymbol{s}} - \boldsymbol{t}_h \boldsymbol{s} \right\|^2_{0,e} \, .$$

On the other hand, applying the boundedness of $\mathbf{I}_h : \mathbf{H}^1(\Omega) \to \mathbf{H}^1(\Omega)$ (cf. [18, Lemma 1.127, pag. 69]), we easily find by the Cauchy-Schwarz and triangle inequalities that

$$\begin{aligned}\Big|\kappa_1 \int_\Omega \boldsymbol{r}_1(\vec{\boldsymbol{t}}_h;\mathbf{0}) : \underline{\mathbf{curl}}(\boldsymbol{\varphi} - \boldsymbol{\varphi}_h)\Big| &\leq \kappa_1 \, \|\boldsymbol{r}_1(\vec{\boldsymbol{t}}_h;\mathbf{0})\|_{0,\Omega} \, |\boldsymbol{\varphi} - \boldsymbol{\varphi}_h|_{1,\Omega} \\ &\leq \kappa_1 \, \|\boldsymbol{r}_1(\vec{\boldsymbol{t}}_h;\mathbf{0})\|_{0,\Omega} \, \Big\{\|\boldsymbol{\varphi}\|_{1,\Omega} + \|\boldsymbol{\varphi}_h\|_{1,\Omega}\Big\} \leq C \, \|\boldsymbol{r}_1(\vec{\boldsymbol{t}}_h;\mathbf{0})\|_{0,\Omega} \, \|\boldsymbol{\varphi}\|_{1,\Omega} \, .\end{aligned} \tag{3.39}$$

In this way, by replacing (3.38) and (3.39) back into (3.35) we arrive at (3.34), thus ending the proof. ∎

Next, we estimate $\big|\, \mathbf{R}_2\big(\nabla \boldsymbol{z} - \Pi_h(\nabla \boldsymbol{z})\big) \,\big|$.

Lemma 3.10 *There exists $C > 0$, independent of h, such that*

$$|\mathbf{R}_2\big(\nabla \boldsymbol{z} - \Pi_h(\nabla \boldsymbol{z})\big)| \leq C \left\{ \sum_{T \in \mathcal{T}_h} \widehat{\theta}^2_{2,T} \right\}^{1/2} \|\boldsymbol{z}\|_{2,\Omega} \, , \tag{3.40}$$

where

$$\begin{aligned}\widehat{\theta}^2_{2,T} := \, & h_T^2 \, \|\boldsymbol{r}_1(\vec{\boldsymbol{t}}_h;\mathbf{0})\|^2_{0,T} + h_T^2 \, \|\boldsymbol{r}_3(\vec{\boldsymbol{t}}_h;\mathbf{0})\|^2_{0,T} + \|\boldsymbol{f} - \mathcal{P}_h\big(\boldsymbol{f}\big)\|^2_{0,T} \\ & + \sum_{e \, \in \, \mathcal{E}(T) \cap \mathcal{E}_h(\Gamma)} h_e \|\boldsymbol{r}_4(\vec{\boldsymbol{t}}_h;\boldsymbol{g})\|^2_{0,e} \, .\end{aligned} \tag{3.41}$$

Proof. Using now the alternative definition of the functional $\mathbf{R}_2$ (cf. (3.22)) we find that

$$\begin{aligned}\mathbf{R}_2\big(\nabla \boldsymbol{z} - \Pi_h(\nabla \boldsymbol{z})\big) \, = \, & \int_\Omega \Big\{ - \kappa_1 \, \boldsymbol{r}_1(\vec{\boldsymbol{t}}_h;\mathbf{0}) + \boldsymbol{r}_3(\vec{\boldsymbol{t}}_h;\mathbf{0}) \Big\} : \big(\nabla \boldsymbol{z} - \Pi_h(\nabla \boldsymbol{z})\big) \\ + \quad & \big\langle \big(\nabla \boldsymbol{z} - \Pi_h(\nabla \boldsymbol{z})\big) \, \boldsymbol{\nu}, \boldsymbol{r}_4(\vec{\boldsymbol{t}}_h;\boldsymbol{g}) \big\rangle - \kappa_2 \int_\Omega \boldsymbol{r}_2(\vec{\boldsymbol{t}}_h;\boldsymbol{f}) \cdot \mathbf{div}\, \big(\nabla \boldsymbol{z} - \Pi_h(\nabla \boldsymbol{z})\big)\end{aligned} \tag{3.42}$$

Then, applying the identity (3.1), denoting by $\mathcal{I}$ a generic identity operator, and using that $\mathbf{div}\, \boldsymbol{\sigma}_h \in \mathbf{P}_k(\mathcal{T}_h)$, we obtain

$$\begin{aligned}\int_\Omega \boldsymbol{r}_2(\vec{\boldsymbol{t}}_h;\boldsymbol{f}) \cdot \mathbf{div}\, \big(\nabla \boldsymbol{z} - \Pi_h(\nabla \boldsymbol{z})\big) \, &= \int_\Omega \boldsymbol{r}_2(\vec{\boldsymbol{t}}_h;\boldsymbol{f}) \cdot \big(\mathcal{I} - \mathcal{P}_h\big)(\mathbf{div}\, \nabla \boldsymbol{z}) \\ &= \int_\Omega \big(\mathcal{I} - \mathcal{P}_h\big)(\boldsymbol{r}_2(\vec{\boldsymbol{t}}_h;\boldsymbol{f})) \cdot \Delta \, \boldsymbol{z} \, = \int_\Omega \big(\boldsymbol{f} - \mathcal{P}_h(\boldsymbol{f})\big) \cdot \Delta \, \boldsymbol{z} \, ,\end{aligned}$$

which yields

$$\left| \int_\Omega \boldsymbol{r}_2(\vec{\boldsymbol{t}}_h;\boldsymbol{f}) \cdot \mathbf{div}\, \big(\nabla \boldsymbol{z} - \Pi_h(\nabla \boldsymbol{z})\big) \right| \leq \|\boldsymbol{f} - \mathcal{P}_h(\boldsymbol{f})\|_{0,\Omega} \, \|\boldsymbol{z}\|_{2,\Omega} \, . \tag{3.43}$$

In turn, the remaining terms on the right hand side of (3.42) are simply bounded by applying the Cauchy-Schwarz inequality in $\mathbb{L}^2(\Omega)$ and $\mathbf{L}^2(\Gamma)$, and then employing the approximation properties of Π_h provided by Lemma 3.2. The resulting estimate together with (3.43) readily lead to (3.40), which ends the proof. ∎

As a straightforward consequence of Lemmas 3.9 and 3.10, the identity (3.32), and the stability estimate of the Helmholtz decomposition (cf. (3.27)), we conclude the required upper bound for $\|\mathbf{R}_2\|_{\mathbb{H}_0(\mathbf{div};\Omega)'}$, that is

$$\|\mathbf{R}_2\|_{\mathbb{H}_0(\mathbf{div};\Omega)'} \,\leq\, C \left\{ \sum_{T\in\mathcal{T}_h} \widetilde{\theta}^2_{2,T} \,+\, \sum_{T\in\mathcal{T}_h} \widehat{\theta}^2_{2,T} \right\}^{1/2} , \tag{3.44}$$

where $C > 0$ is a constant independent of h.

We are now ready to establish the reliability estimate for $\boldsymbol{\theta}_2$.

Theorem 3.11 *Assume that the data satisfy* (3.6)*, and let* $\vec{\boldsymbol{t}} \in \mathbf{H}$ *and* $\vec{\boldsymbol{t}}_h \in \mathbf{H}_h$ *be the unique solutions of the continuous and discrete formulations* (2.7) *and* (2.10)*, respectively. Then there exists* $c_{\mathtt{rel}} > 0$*, independent of* h*, such that*

$$\|\vec{\boldsymbol{t}} - \vec{\boldsymbol{t}}_h\| \,\leq\, c_{\mathtt{rel}}\, \boldsymbol{\theta}_2 \,. \tag{3.45}$$

Proof. Having in mind the general estimate provided by (3.9) (cf. Lemma 3.5), we begin by recalling, as announced before, that the reliability of $\boldsymbol{\theta}_2$ arises from the same upper bounds of $\|\mathbf{R}_1\|_{\mathbb{L}^2_{\mathtt{tr}}(\Omega)'}$ and $\|\mathbf{R}_3\|_{\mathbf{H}^1(\Omega)'}$ given in (3.24) and (3.25), respectively, together with the new estimate of $\|\mathbf{R}_2\|_{\mathbb{H}_0(\mathbf{div};\Omega)'}$ provided by (3.44). In this way, and observing that the terms $h_T^2\,\|\boldsymbol{r}_1(\vec{\boldsymbol{t}}_h;\mathbf{0})\|^2_{0,T}$, $h_T^2\,\|\boldsymbol{r}_3(\vec{\boldsymbol{t}}_h;\mathbf{0})\|^2_{0,T}$, and $h_e\|\boldsymbol{r}_4(\vec{\boldsymbol{t}}_h;\boldsymbol{g})\|^2_{0,e}$, which form part of $\widehat{\theta}^2_{2,T}$ (cf. (3.41)), are dominated by $\|\boldsymbol{r}_1(\vec{\boldsymbol{t}}_h;\mathbf{0})\|^2_{0,T}$, $\|\boldsymbol{r}_3(\vec{\boldsymbol{t}}_h;\mathbf{0})\|^2_{0,T}$, and $\|\boldsymbol{r}_4(\vec{\boldsymbol{t}}_h;\boldsymbol{g})\|^2_{0,e}$, respectively, which appear in the aforementioned bounds, we conclude (3.45) after replacing (3.24), (3.25), and (3.44) back into (3.9).

∎

3.5 Efficiency of the a posteriori error estimators

In this section we prove the lower estimates announced in (3.7) (cf. Theorem 3.3) and (3.8) (cf. Theorem 3.4). Most of the corresponding analysis consists of deriving suitable upper bounds depending on the true errors for each one of the terms defining the local error indicators $\theta^2_{1,T}$ and $\theta^2_{2,T}$. For this purpose, we make extensive use of the original system of equations (2.6), which is recovered from the augmented continuous formulation (2.7) by choosing suitable test functions and integrating by parts backwardly the corresponding equations.

We begin with the efficiency estimate for $\boldsymbol{\theta}_1$.

Theorem 3.12 *Let* $\vec{\boldsymbol{t}} \in \mathbf{H}$ *and* $\vec{\boldsymbol{t}}_h \in \mathbf{H}_h$ *be the unique solutions of the continuous and discrete formulations* (2.7) *and* (2.10)*, respectively. Then there exists* $C_{\mathtt{eff}} > 0$*, independent of* h*, such that*

$$C_{\mathtt{eff}}\, \boldsymbol{\theta}_1 \,\leq\, \|\vec{\boldsymbol{t}} - \vec{\boldsymbol{t}}_h\| \,. \tag{3.46}$$

Proof. We first deduce from (3.2) and the second equation of (2.6) that

$$\boldsymbol{r}_1(\vec{\boldsymbol{t}}_h;\mathbf{0}) \,=\, \big(\boldsymbol{\sigma}_h^{\mathtt{d}} \,-\, \boldsymbol{\sigma}^{\mathtt{d}}\big) \,-\, \big(\mu(|\boldsymbol{t}_h|)\,\boldsymbol{t}_h \,-\, \mu(|\boldsymbol{t}|)\,\boldsymbol{t}\big) \,+\, \big((\boldsymbol{u}_h\otimes\boldsymbol{u}_h)^{\mathtt{d}} \,-\, (\boldsymbol{u}\otimes\boldsymbol{u})^{\mathtt{d}}\big)\,,$$

which, applying (2.3) (cf. Lemma 2.1), and noting that $\|\boldsymbol{\tau}^{\mathtt{d}}\|_{0,\Omega} \,\leq\, \|\boldsymbol{\tau}\|_{0,\Omega}$ for each $\boldsymbol{\tau}\in\mathbb{L}^2(\Omega)$, yields

$$\|\boldsymbol{r}_1(\vec{\boldsymbol{t}}_h;\mathbf{0})\|^2_{0,\Omega} \,\leq\, 3\Big\{\|\boldsymbol{\sigma}_h \,-\, \boldsymbol{\sigma}\|^2_{0,\Omega} \,+\, L_\mu^2\,\|\,\boldsymbol{t} - \boldsymbol{t}_h\|^2_{0,\Omega} \,+\, \|(\boldsymbol{u}_h\otimes\boldsymbol{u}_h) \,-\, (\boldsymbol{u}\otimes\boldsymbol{u})\|^2_{0,\Omega}\Big\}\,. \tag{3.47}$$

In turn, subtracting and adding $\boldsymbol{u}$ in the first term involving the tensor product $\otimes$, and using Cauchy-Schwarz's inequality for the resulting expressions, we find that

$$\|(\boldsymbol{u}_h \otimes \boldsymbol{u}_h) \,-\, (\boldsymbol{u} \otimes \boldsymbol{u})\|^2_{0,\Omega} \,\leq\, 2\left\{\|\boldsymbol{u}_h\|^2_{\mathbf{L}^4(\Omega)} \,+\, \|\boldsymbol{u}\|^2_{\mathbf{L}^4(\Omega)}\right\}\|\boldsymbol{u} - \boldsymbol{u}_h\|^2_{\mathbf{L}^4(\Omega)}\,,$$

from which, employing that the injection $\mathbf{i}_c : \mathbf{H}^1(\Omega) \to \mathbf{L}^4(\Omega)$ is compact (and hence continuous) (see Rellich-Kondrachov compactness Theorem in [1, Theorem 6.3] or [36, Theorem 1.3.5]), and using from [11, Theorems 3.9 and 4.2] that $\|\boldsymbol{u}\|_{1,\Omega}$ and $\|\boldsymbol{u}_h\|_{1,\Omega}$ are bounded above by ρ_0 (cf. (2.8)), we deduce that

$$\|(\boldsymbol{u}_h \otimes \boldsymbol{u}_h) \,-\, (\boldsymbol{u} \otimes \boldsymbol{u})\|^2_{0,\Omega} \,\leq\, 4\,\rho_0^2\,\|\mathbf{i}_c\|^4\,\|\boldsymbol{u} - \boldsymbol{u}_h\|^2_{1,\Omega}\,. \tag{3.48}$$

On the other hand, it is readily seen from (3.2) and the remaining equations of (2.6) that

$$\begin{aligned}
\|\boldsymbol{r}_2(\vec{\boldsymbol{t}}_h;\boldsymbol{f})\|^2_{0,\Omega} \,&\leq\, \|\mathbf{div}\,(\boldsymbol{\sigma} \,-\, \boldsymbol{\sigma}_h)\|^2_{0,\Omega}\,,\\
\|\boldsymbol{r}_3(\vec{\boldsymbol{t}}_h;\boldsymbol{0})\|^2_{0,\Omega} \,&\leq\, 2\left\{|\boldsymbol{u} \,-\, \boldsymbol{u}_h|^2_{1,\Omega} \,+\, \|\boldsymbol{t} \,-\, \boldsymbol{t}_h\|^2_{0,\Omega}\right\},\\
\|\boldsymbol{r}_4(\vec{\boldsymbol{t}}_h;\boldsymbol{g})\|^2_{0,\Gamma} \,&\leq\, C\,\|\boldsymbol{u} \,-\, \boldsymbol{u}_h\|^2_{1,\Omega}\,,
\end{aligned}$$

and

$$\|\boldsymbol{r}_4(\vec{\boldsymbol{t}}_h;\boldsymbol{g})\|^2_{1/2,\Gamma} \,\leq\, C\,\|\boldsymbol{u} \,-\, \boldsymbol{u}_h\|^2_{1,\Omega}\,, \tag{3.49}$$

where the last two inequalities make use of the trace inequalities in $\mathbf{L}^2(\Gamma)$ and $\mathbf{H}^{1/2}(\Gamma)$, respectively. In this way, the required efficiency estimate (3.46) follows straightforwardly from the definition of $\boldsymbol{\theta}_1$ (cf. (3.5)) and the inequalities (3.47), (3.48) – (3.49).

∎

We now aim to establish the efficiency of $\boldsymbol{\theta}_2$. More precisely, thanks to the previous theorem, it only remains to prove the corresponding upper bounds for the other four terms defining $\theta^2_{2,T}$ (cf. (3.4)). For this purpose, we proceed as in [13, 24, 4], and apply the localization technique based on triangle-bubble and edge-bubble functions, together with extension operators, discrete trace and inverse inequalities. According to the above, we now introduce additional notations and preliminary results. Given $T \in \mathcal{T}_h$ and $e \in \mathcal{E}(T)$, we let ψ_T and ψ_e be the usual triangle-bubble and edge-bubble functions, respectively (see [38, eqs. (1.5) and (1.6)]), for which there hold:

i) $\psi_T \in P_{n+1}(T)$, $\psi_T = 0$ on ∂T, $\mathrm{supp}(\psi_T) \subseteq T$, and $0 \leq \psi_T \leq 1$ in T.

ii) $\psi_e|_T \in P_n(T)$, $\psi_e = 0$ on $\partial T \setminus e$, $\mathrm{supp}(\psi_e) \subseteq w_e := \cup\{T' \in \mathcal{T}_h : \; e \in \mathcal{E}(T')\}$, and $0 \leq \psi_e \leq 1$ in w_e.

It is well-known that, given $k \in \mathbb{N} \cup \{0\}$, there exists an extension operator $L : C(e) \to C(T)$ that satisfies $L(p) \in P_k(T)$ and $L(p)|_e = p$ for all $p \in P_k(e)$. Further properties of ψ_T, ψ_e and L are stated in the following lemma (see e.g. [38]).

Lemma 3.13 *Given $k \in \mathbb{N} \cup \{0\}$, there exist positive constants c_1, c_2, and c_3, depending only on k and the shape regularity of the triangulations (minimum angle condition), such that for each $T \in \mathcal{T}_h$ and $e \in \mathcal{E}(T)$, there hold*

$$\|p\|^2_{0,e} \,\leq\, c_2\|\psi_e^{1/2}p\|^2_{0,e} \qquad \forall p \in P_k(e)\,,$$

and

$$\|\psi_e^{1/2}L(p)\|^2_{0,T} \,\leq\, c_3\,h_e\|p\|^2_{0,e} \qquad \forall p \in P_k(e)\,.$$

The following inverse and discrete trace inequalities are also employed.

Lemma 3.14 *Let k, l, $m \in \mathbb{N} \cup \{0\}$ such that $l \leq m$. Then there exists $c > 0$, depending only on k, l, m and the shape regularity of the triangulations, such that for each $T \in \mathcal{T}_h$ there holds*

$$|q|_{m,T} \leq c\, h_T^{l-m}\, |q|_{l,T} \qquad \forall\, q \in P_k(T)\,.$$

Proof. See [14, Theorem 3.2.6].

∎

Lemma 3.15 *There exists $C > 0$, depending only on the shape regularity of the triangulations, such that for each $T \in \mathcal{T}_h$ and $e \in \mathcal{E}(T)$, there holds*

$$\|v\|_{0,e}^2 \leq C \left\{ h_e^{-1}\, \|v\|_{0,T}^2 + h_e\, |v|_{1,T}^2 \right\} \quad \forall\, v \in H^1(T)\,.$$

Proof. See [2, Theorem 3.10].

∎

In turn, the following lemma, whose proof makes use of Lemmas 3.13 and 3.14, is applied next to bound the terms involving **curl** and the tangential jumps across the edges of $\mathcal{T}_h$.

Lemma 3.16 *Let $\boldsymbol{\rho}_h \in \mathbb{L}^2(\Omega)$ be a piecewise polynomial tensor of degree $k \geq 0$ on each $T \in \mathcal{T}_h$, and let $\boldsymbol{\rho} \in \mathbb{L}^2(\Omega)$ be such that $\mathbf{curl}(\boldsymbol{\rho}) = 0$ in Ω. Then, there exist c, $\widetilde{c} > 0$, independent of h, such that*

$$\|\mathbf{curl}(\boldsymbol{\rho}_h)\|_{0,T} \leq c\, h_T^{-1}\, \|\boldsymbol{\rho} - \boldsymbol{\rho}_h\|_{0,T} \qquad \forall\, T \in \mathcal{T}_h\,, \tag{3.50}$$

and

$$\|[\boldsymbol{\rho}_h \boldsymbol{s}]\|_{0,e} \leq \widetilde{c}\, h_e^{-1/2}\, \|\boldsymbol{\rho} - \boldsymbol{\rho}_h\|_{0,\omega_e} \qquad \forall\, e \in \mathcal{E}_h(\Omega)\,. \tag{3.51}$$

Proof. For the proof of (3.50) we refer to [7, Lemma 4.3], whereas (3.51) is a slight modification of the proof of [7, Lemma 4.4]. We omit further details.

∎

The following lemma provides the required upper bounds for the second and fourth terms on the right hand side of (3.4).

Lemma 3.17 *There exists C_1, $C_2 > 0$, independent of h, such that*

$$h_T^2 \big\|\mathbf{curl}(\boldsymbol{t}_h)\big\|_{0,T}^2 \leq C_1\, \|\boldsymbol{t} - \boldsymbol{t}_h\|_{0,T}^2 \qquad \forall\, T \in \mathcal{T}_h\,,$$

and

$$h_e\, \big\|\big[\boldsymbol{t}_h\, \boldsymbol{s}\big]\big\|_{0,e}^2 \leq C_2\, \|\boldsymbol{t} - \boldsymbol{t}_h\|_{0,w_e}^2 \qquad \forall\, e \in \mathcal{E}_h(\Omega)\,.$$

Proof. It suffices to apply Lemma 3.16 with $\boldsymbol{\rho}_h = \boldsymbol{t}_h$ and $\boldsymbol{\rho} = \boldsymbol{t} = \nabla \boldsymbol{u}$.

∎

Now, the third and fifth terms on the right hand side of (3.4) are estimated as follows.

Lemma 3.18 *There holds*

$$\|\boldsymbol{f} - \mathcal{P}_h(\boldsymbol{f})\|_{0,T} \leq 2\, \|\mathbf{div}\, \boldsymbol{\sigma} - \mathbf{div}\, \boldsymbol{\sigma}_h\|_{0,T} \qquad \forall\, T \in \mathcal{T}_h\,. \tag{3.52}$$

Proof. Using that $\boldsymbol{f} = -\mathbf{div}\,\boldsymbol{\sigma}$, and then adding and subtracting $\mathcal{P}_h(\mathbf{div}\,\boldsymbol{\sigma}_h) = \mathbf{div}\,\boldsymbol{\sigma}_h$, we readily find that

$$\|\boldsymbol{f} - \mathcal{P}_h(\boldsymbol{f})\|_{0,T} \leq \|\mathcal{P}_h\big(\mathbf{div}\,\boldsymbol{\sigma} - \mathbf{div}\,\boldsymbol{\sigma}_h\big)\|_{0,T} + \|\mathbf{div}\,\boldsymbol{\sigma}_h - \mathbf{div}\,\boldsymbol{\sigma}\|_{0,T}\,,$$

which yields (3.52) and ends the proof. ∎

Lemma 3.19 *There exists $C_3 > 0$, independent of h, such that*

$$h_e \left\| \frac{d\boldsymbol{g}}{d\boldsymbol{s}} - \boldsymbol{t}_h \boldsymbol{s} \right\|^2_{0,e} \leq C_3 \, \|\boldsymbol{t} - \boldsymbol{t}_h\|^2_{0,T_e} \qquad \forall\, e \in \mathcal{E}_h(\Gamma)\,,$$

where T_e is the triangle of $\mathcal{T}_h$ having e as and edge.

Proof. It follows similarly to the proof of [26, Lemma 4.15]. We omit further details. ∎

As a consequence of Theorem 3.12 and Lemmas 3.17, 3.18, and 3.19, we are now in position to state the efficiency of $\boldsymbol{\theta}_2$.

Theorem 3.20 *Let $\vec{\boldsymbol{t}} \in \mathbf{H}$ and $\vec{\boldsymbol{t}}_h \in \mathbf{H}_h$ be the unique solutions of the continuous and discrete formulations* (2.7) *and* (2.10)*, respectively. Then there exists $c_{\mathtt{eff}} > 0$, independent of h, such that*

$$c_{\mathtt{eff}}\, \boldsymbol{\theta}_2 \leq \|\vec{\boldsymbol{t}} - \vec{\boldsymbol{t}}_h\|\,.$$

4 A posteriori error analysis: The 3D case

In this section we extend the results from Section 3 to the three-dimensional version of (2.10). Similarly as in Section 3, given a tetrahedron $T \in \mathcal{T}_h$, we let $\mathcal{E}(T)$ be the set of its faces, and let $\mathcal{E}_h$ be the set of all faces of the triangulation $\mathcal{T}_h$. Then, we write $\mathcal{E}_h = \mathcal{E}_h(\Omega) \cup \mathcal{E}_h(\Gamma)$, where $\mathcal{E}_h(\Omega) := \{e \in \mathcal{E}_h : \ e \subseteq \Omega\}$ and $\mathcal{E}_h(\Gamma) := \{e \in \mathcal{E}_h : \ e \subseteq \Gamma\}$. Also, for each face $e \in \mathcal{E}_h$ we fix a unit normal $\boldsymbol{\nu}_e$ to e, so that given $\boldsymbol{\tau} \in \mathbb{L}^2(\Omega)$ such that $\boldsymbol{\tau}|_T \in \mathbb{C}(T)$ on each $T \in \mathcal{T}_h$, and given $e \in \mathcal{E}_h(\Omega)$, we let $\big[\boldsymbol{\tau} \times \boldsymbol{\nu}_e\big]$ be the corresponding jump of the tangential traces across e, that is $\big[\boldsymbol{\tau} \times \boldsymbol{\nu}_e\big] := (\boldsymbol{\tau}|_T - \boldsymbol{\tau}|_{T'})|_e \times \boldsymbol{\nu}_e$, where T and T' are the elements of $\mathcal{T}_h$ having e as a common face. In what follows, when no confusion arises, we simple write $\boldsymbol{\nu}$ instead of $\boldsymbol{\nu}_e$.

Now, we recall that the curl of a 3D vector $\boldsymbol{v} := (v_1, v_2, v_3)$ is the 3D vector

$$\mathrm{curl}(\boldsymbol{v}) \;=\; \nabla \times \boldsymbol{v} \;:=\; \left(\frac{\partial v_3}{\partial x_2} - \frac{\partial v_2}{\partial x_3}\,,\; \frac{\partial v_1}{\partial x_3} - \frac{\partial v_3}{\partial x_1}\,,\; \frac{\partial v_2}{\partial x_1} - \frac{\partial v_1}{\partial x_2} \right),$$

and that, given a tensor function $\boldsymbol{\tau} := (\tau_{ij})_{3\times 3}$, the operator $\underline{\mathbf{curl}}$ denotes curl acting along each row of $\boldsymbol{\tau}$, that is, $\underline{\mathbf{curl}}(\boldsymbol{\tau})$ is the 3×3 tensor whose rows are given by

$$\underline{\mathbf{curl}}(\boldsymbol{\tau}) \;:=\; \begin{pmatrix} \mathrm{curl}(\tau_{11}, \tau_{12}, \tau_{13}) \\ \mathrm{curl}(\tau_{21}, \tau_{22}, \tau_{23}) \\ \mathrm{curl}(\tau_{31}, \tau_{32}, \tau_{33}) \end{pmatrix}.$$

In addition, $\boldsymbol{\tau} \times \boldsymbol{\nu}$ stands for the 3×3 tensor whose rows are given by the tangential components of each row of $\boldsymbol{\tau}$, that is,

$$\boldsymbol{\tau} \times \boldsymbol{\nu} \;:=\; \begin{pmatrix} (\tau_{11}, \tau_{12}, \tau_{13}) \times \boldsymbol{\nu} \\ (\tau_{21}, \tau_{22}, \tau_{23}) \times \boldsymbol{\nu} \\ (\tau_{31}, \tau_{32}, \tau_{33}) \times \boldsymbol{\nu} \end{pmatrix}.$$

Having introduced these notations, and employing the same definitions of the residuals given in (3.2), we now set for each $T \in \mathcal{T}_h$ the local a posteriori error indicators $\theta^2_{1,T}$ (exactly as in (3.3)), and

$$\begin{aligned}\theta^2_{2,T} \,:=\, \theta^2_{1,T} \,+\, h_T^2 \|\underline{\mathbf{curl}}(\boldsymbol{t}_h)\|^2_{0,T} \,+\, \|\boldsymbol{f} - \mathcal{P}_h(\boldsymbol{f})\|^2_{0,T} \\ +\, \sum_{e\,\in\,\mathcal{E}(T)\cap\mathcal{E}_h(\Omega)} h_e \left\|\left[\boldsymbol{t}_h \times \boldsymbol{\nu}\right]\right\|^2_{0,e} \,+\, \sum_{e\,\in\,\mathcal{E}(T)\cap\mathcal{E}_h(\Gamma)} h_e \,\|\nabla \boldsymbol{g} \times \boldsymbol{\nu} \,-\, \boldsymbol{t}_h \times \boldsymbol{\nu}\|^2_{0,e}\,. \end{aligned} \tag{4.1}$$

In this way, the corresponding global a posteriori error estimators are defined as in (3.5), that is

$$\boldsymbol{\theta}_1 \,:=\, \left\{\sum_{T\in\mathcal{T}_h} \theta^2_{1,T} \,+\, \|\boldsymbol{r}_4(\vec{\boldsymbol{t}}_h;\boldsymbol{g})\|^2_{1/2,\Gamma}\right\}^{1/2} \quad \text{and} \quad \boldsymbol{\theta}_2 \,:=\, \left\{\sum_{T\in\mathcal{T}_h} \theta^2_{2,T}\right\}^{1/2},$$

and the main estimates, which are the analogue of Theorems 3.3 and 3.4, are stated as follows.

Theorem 4.1 *Assume that $\boldsymbol{f} \in \mathbf{L}^\infty(\Omega)$ and $\boldsymbol{g} \in \mathbf{H}^1(\Gamma)$, and that there holds (3.6). In addition, let $\vec{\boldsymbol{t}} \in \mathbf{H}$ and $\vec{\boldsymbol{t}}_h \in \mathbf{H}_h$ be the unique solutions of the continuous and discrete formulations (2.7) and (2.10), respectively. Then, there exist constants $C_{\mathtt{rel}} > 0$, $C_{\mathtt{eff}} > 0$, $c_{\mathtt{rel}} > 0$, and $c_{\mathtt{eff}} > 0$, independent of h, such that*

$$C_{\mathtt{eff}}\,\boldsymbol{\theta}_1 \,\leq\, \|\vec{\boldsymbol{t}} - \vec{\boldsymbol{t}}_h\| \,\leq\, C_{\mathtt{rel}}\,\boldsymbol{\theta}_1\,.$$

and

$$c_{\mathtt{eff}}\,\boldsymbol{\theta}_2 \,\leq\, \|\vec{\boldsymbol{t}} - \vec{\boldsymbol{t}}_h\| \,\leq\, c_{\mathtt{rel}}\,\boldsymbol{\theta}_2\,.$$

The proof of Theorem 4.1 follows very closely the analysis of Section 3, except a few issues to be described throughout the following discussion. Indeed, we first observe that the general a posteriori error estimate given by Lemma 3.5 is also valid in 3D, and that the corresponding upper bounds of $\|\mathbf{R}_1\|_{\mathbb{L}^2_{\mathrm{tr}}(\Omega)'}$, $\|\mathbf{R}_3\|_{\mathbf{H}^1(\Omega)'}$, and $\|\mathbf{R}_2\|_{\mathbb{H}_0(\mathbf{div};\Omega)'}$ yielding the reliability of $\boldsymbol{\theta}_1$ are the same as those given in (3.24), (3.25), and (3.26), respectively.

In turn, for the reliability of $\boldsymbol{\theta}_2$, we need to use a 3D version of the stable Helmholtz decomposition provided by Lemma 3.7, which is valid only for 2D. This required result and a further extension of it to a particular case of Neumann boundary conditions were established recently for arbitrary polyhedral domains in [23, Theorem 3.1]. Before it, the stability of the Helmholtz decomposition in 3D was known only for convex regions (see, e.g. [40, Proposition 4.52]), whose proof is consequence of some results from [5]. We remark that the analysis in [23] also makes use of several estimates available in [5]. Next, the associated discrete Helmholtz decomposition and the functional $\mathbf{R}_2$ are set and rewritten exactly as in (3.31) and (3.32), respectively. Furthermore, in order to derive the new upper bound of $\|\mathbf{R}_2\|_{\mathbb{H}_0(\mathbf{div};\Omega)'}$, we now need the 3D analogue of the integration by parts formula on the boundary given by (3.33) (cf. Lemma 3.8). In fact, by applying again the identities from [29, Chapter I, eq. (2.17) and Theorem 2.11], we deduce that in this case there holds

$$\langle \underline{\mathbf{curl}}\,\boldsymbol{\chi}\,\boldsymbol{\nu}, \boldsymbol{\phi}\rangle \,=\, -\,\langle \nabla\boldsymbol{\phi} \times \boldsymbol{\nu}, \boldsymbol{\chi}\rangle \qquad \forall\,\boldsymbol{\chi} \,\in\, \mathbb{H}^1(\Omega)\,, \quad \forall\,\boldsymbol{\phi} \,\in\, \mathbf{H}^1(\Omega)\,.$$

In addition, the integration by parts formula on each tetrahedron $T \in \mathcal{T}_h$, which is employed in the proof of the 3D analogue of Lemma 3.9, becomes (cf. [29, Chapter I, Theorem 2.11])

$$\int_T \underline{\mathbf{curl}}\,\boldsymbol{\tau} : \boldsymbol{\chi} \,-\, \int_T \boldsymbol{\tau} : \underline{\mathbf{curl}}\,\boldsymbol{\chi} \,=\, \langle \boldsymbol{\tau} \times \boldsymbol{\nu}, \boldsymbol{\chi}\rangle_{\partial T} \qquad \forall\,\boldsymbol{\tau} \in \mathbb{H}(\underline{\mathbf{curl}};\Omega)\,, \quad \forall\,\boldsymbol{\chi} \in \mathbb{H}^1(\Omega)\,,$$

where $\langle\cdot,\cdot\rangle_{\partial T}$ is the duality pairing between $\mathbb{H}^{-1/2}(T)$ and $\mathbb{H}^{1/2}(T)$, and, as usual, $\mathbb{H}(\underline{\mathbf{curl}};\Omega)$ is the space of tensors in $\mathbb{L}^2(\Omega)$ whose $\underline{\mathbf{curl}}$ lie also in $\mathbb{L}^2(\Omega)$. Note that the foregoing identities explain the

D.o.f.	h	$e(\boldsymbol{t})$	$r(\boldsymbol{t})$	$e(\boldsymbol{\sigma})$	$r(\boldsymbol{\sigma})$	$e(\boldsymbol{u})$	$r(\boldsymbol{u})$	$\mathtt{eff}(\boldsymbol{\theta}_1)$	$\mathtt{eff}(\boldsymbol{\theta}_2)$	iter
Augmented $\mathbb{P}_0 - \mathbb{RT}_0 - \mathbf{P}_1$ scheme										
74	1.4142	4.7503	–	91.5264	–	11.5238	–	1.0219	0.6711	4
258	0.7071	3.1161	0.6082	53.1640	0.7837	5.2062	1.1462	1.0093	0.6720	5
962	0.3535	1.5991	0.9624	32.6029	0.7054	2.6013	1.0009	1.0073	0.6732	5
3714	0.1767	0.8003	0.9986	17.7405	0.8779	1.2612	1.0443	1.0069	0.6778	5
14594	0.0883	0.3986	1.0055	8.9096	0.9936	0.6210	1.0221	1.0070	0.6828	4
57858	0.0441	0.1990	1.0021	4.4821	0.9911	0.3090	1.0070	1.0069	0.6849	5
230402	0.0220	0.0994	1.0007	2.2497	0.9944	0.1542	1.0019	1.0069	0.6856	5
919554	0.0110	0.0497	1.0002	1.1259	0.9985	0.0771	1.0005	1.0069	0.6858	5
Augmented $\mathbb{P}_1 - \mathbb{RT}_1 - \mathbf{P}_2$ scheme										
173	1.4142	3.9997	–	73.6908	–	5.4413	–	0.9627	0.2804	5
589	0.7071	1.7202	1.2172	30.2571	1.4738	2.0013	1.4429	0.9792	0.2899	5
2165	0.3535	0.3219	2.4176	12.1352	1.3180	0.4759	2.0720	0.9790	0.2939	5
8293	0.1767	0.0734	2.1328	4.7582	1.7127	0.1125	2.0797	0.9807	0.2964	5
32453	0.0883	0.0184	1.9905	1.2888	1.8223	0.0260	2.1110	0.9794	0.3030	5
128389	0.0441	0.0048	1.9320	0.3577	1.8492	0.0064	1.9940	0.9799	0.3016	5
510725	0.0220	0.0012	1.9834	0.0913	1.9691	0.0016	1.9944	0.9788	0.2996	6
2037253	0.0110	0.0003	1.9987	0.0227	1.9786	0.0004	1.9953	0.9800	0.2996	5

Table 5.1: Test 1: convergence history and Newton iteration count for the $\mathbb{P}_k - \mathbb{RT}_k - \mathbf{P}_{k+1}$ approximations of the Navier–Stokes problem, with $k = 0, 1$.

appearing of the expressions $\boldsymbol{t}_h \times \boldsymbol{\nu}$ and $\nabla \boldsymbol{g} \times \boldsymbol{\nu} - \boldsymbol{t}_h \times \boldsymbol{\nu}$ in the 3D definition of $\theta^2_{2,T}$ (cf. (4.1)). The rest of the proof of the reliability of $\boldsymbol{\theta}_2$ and the entire analysis yielding the efficiency of both $\boldsymbol{\theta}_1$ and $\boldsymbol{\theta}_2$ proceed as in Sections 3.4 and 3.5, respectively. Just for sake of completeness, we remark that most of the details concerning the 3D version of the efficiency estimates given in Lemmas 3.16, 3.17, and 3.19, can be found in (or derived from) [25, Lemmas 4.9, 4.10, 4.11, and 4.13].

5 Numerical results

We numerically investigate the performance and accuracy of the proposed augmented finite element scheme along with the properties of the a posteriori error estimators $\boldsymbol{\theta}_1$ and $\boldsymbol{\theta}_2$ derived in Section 3 and 4, respectively. In this regard, we remark that for purposes of adaptivity, which requires to have locally computable indicators, we now use that

$$\|\boldsymbol{r}_4(\vec{\boldsymbol{t}}_h;\boldsymbol{g})\|^2_{1/2,\Gamma} \,\leq\, c\,\|\boldsymbol{r}_4(\vec{\boldsymbol{t}}_h;\boldsymbol{g})\|^2_{1,\Gamma} \,=\, c \sum_{e\,\in\,\mathcal{E}_h(\Gamma)} \|\boldsymbol{r}_4(\vec{\boldsymbol{t}}_h;\boldsymbol{g})\|^2_{1,e}\,,$$

and redefine $\boldsymbol{\theta}_1$ as

$$\boldsymbol{\theta}_1 \,:=\, \Big\{ \sum_{T\in\mathcal{T}_h} \theta^2_{1,T} \Big\}^{1/2}\,,$$

where

$$\theta^2_{1,T} \,:=\, \|\boldsymbol{r}_1(\vec{\boldsymbol{t}}_h;\boldsymbol{0})\|^2_{0,T} \,+\, \|\boldsymbol{r}_2(\vec{\boldsymbol{t}}_h;\boldsymbol{f})\|^2_{0,T} \,+\, \|\boldsymbol{r}_3(\vec{\boldsymbol{t}}_h;\boldsymbol{0})\|^2_{0,T} \,+ \sum_{e\,\in\,\mathcal{E}(T)\cap\mathcal{E}_h(\Gamma)} \|\boldsymbol{r}_4(\vec{\boldsymbol{t}}_h;\boldsymbol{g})\|^2_{1,e}\,.$$

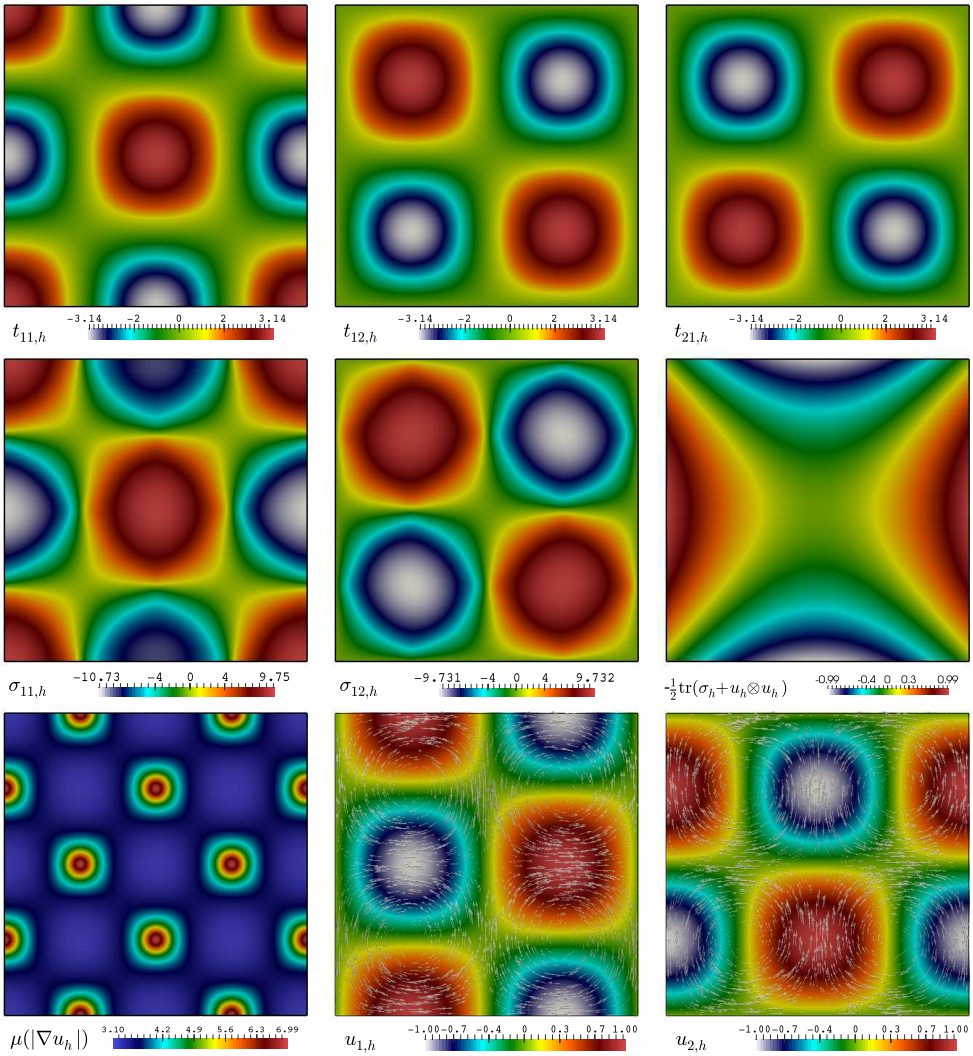

Figure 5.1: Test 1: $\mathbb{P}_1-\mathbb{RT}_1-\mathbf{P}_2$ approximation of velocity gradient components (top panels), Cauchy stress first components and postprocessed pressure field (center panels), and viscosity with velocity components and vector directions (bottom row).

Under this redefinition $\boldsymbol{\theta}_1$ is certainly still reliable, but efficient only up to all its terms, except for the last one, associated to the boundary Γ. Nevertheless, the numerical results to be displayed below allow us to conjecture that this modified $\boldsymbol{\theta}_1$ actually verifies both properties. Furthermore, a Newton-Raphson procedure is employed to linearise (2.9) (where we recall that the convective term is already linearised via a fixed-point strategy), and impose a fixed tolerance of 1E-6 on the norm of the incremental solutions. Linear systems were solved with the iterative GMRES method preconditioned with a multilevel incomplete-LU factorisation. In all subsequent cases, the viscosity is set as

$$\mu(s) := \alpha_0 + \alpha_1(1+s^2)^{-1/2}, \quad \mu_1 = \alpha_0 < \mu(s) < \alpha_1 = \mu_2, \quad \text{for } s \geq 0,$$

and the stabilisation coefficients are chosen according to their optimal values suggested by the analysis of Section 2, that is, $L_\mu = \max\{\mu_2, 2\mu_2 - \mu_1\}$, $\delta = L_\mu^{-1}$, $\kappa_1 = \delta\mu_1/L_\mu$, $\kappa_2 = \kappa_1$, $\kappa_3 = \mu_1 - \frac{\kappa_1 L_\mu}{2\delta}$, $\kappa_4 = \mu_1/4$. In addition, the mean value of $\mathrm{tr}\,\boldsymbol{\sigma}_h$ over Ω is fixed via a penalisation strategy.

D.o.f.	$e(\boldsymbol{t})$	$r(\boldsymbol{t})$	$e(\boldsymbol{\sigma})$	$r(\boldsymbol{\sigma})$	$e(\boldsymbol{u})$	$r(\boldsymbol{u})$	$e(p)$	$r(p)$	e	r	iter	eff($\boldsymbol{\theta}_i$)
Augmented $\mathbb{P}_0 - \mathbb{RT}_0 - \mathbf{P}_1$ scheme with uniform refinement												
794	6.3200	–	450.6412	–	11.0093	–	17.2742	–	450.8528	–	6	–
1876	5.1547	0.4741	413.9833	0.1953	7.7599	0.8135	14.6693	0.3802	414.0881	0.1946	5	–
4880	4.4945	0.2867	386.1393	0.1456	5.2116	0.8327	9.9066	0.8212	386.2006	0.1458	6	–
15480	2.8735	0.7749	260.9739	0.6787	3.8975	0.7170	6.9631	0.6108	261.0058	0.6788	6	–
55622	1.8025	0.7291	177.1064	0.6061	2.2694	0.7904	3.7081	0.9852	177.1201	0.6062	6	–
206242	1.1616	0.7588	98.3499	0.7977	1.4177	0.6963	2.2597	0.7558	98.3555	0.7977	7	–
799732	0.8884	0.7997	51.9209	0.9114	1.0376	0.7494	1.1785	0.8915	53.9234	0.8714	7	–
Augmented $\mathbb{P}_0 - \mathbb{RT}_0 - \mathbf{P}_1$ scheme with adaptive refinement via $\boldsymbol{\theta}_1$												
638	4.5173	–	411.7368	–	7.9698	–	16.911	–	411.8387	–	6	1.0013
1308	3.0896	1.0582	339.4973	0.5374	4.2947	1.4880	7.5044	2.2634	339.5373	0.5378	6	1.0007
2418	1.8071	1.7456	168.9206	2.2721	3.2822	1.4399	4.2425	1.8564	168.9419	1.5720	6	1.0009
6199	0.8863	1.5134	80.7837	1.5670	1.5660	1.2590	2.4891	1.1328	80.7932	1.3670	5	1.0012
21914	0.5149	0.9601	34.9716	1.3260	0.9218	1.0924	1.2172	1.1302	34.9793	1.2259	5	1.0018
110799	0.2231	1.0321	14.6106	1.0771	0.3215	1.0573	0.5409	1.0008	14.6140	1.0771	6	1.0020
668283	0.0940	0.9614	5.8537	1.0180	0.1245	1.0072	0.2217	0.9927	5.8552	1.0179	6	1.0022
Augmented $\mathbb{P}_0 - \mathbb{RT}_0 - \mathbf{P}_1$ scheme with adaptive refinement via $\boldsymbol{\theta}_2$												
615	4.3007	–	402.5308	–	7.3464	–	16.1987	–	402.6208	–	6	0.6988
1243	2.9774	1.0451	320.5792	0.6597	4.3928	1.4616	8.6691	1.7768	330.6218	0.5599	6	0.7001
2614	1.6849	1.5318	165.1663	1.4669	1.8411	2.3396	4.0207	2.0671	165.1852	1.8669	6	0.7041
6529	0.8727	1.4373	76.9355	1.3692	0.8917	1.5838	2.3679	1.1567	76.9456	1.3691	6	0.7045
24145	0.4898	0.9832	33.0832	1.2906	0.4837	0.9553	1.1645	1.0852	33.0904	1.2904	6	0.7038
126045	0.2138	1.0030	13.3836	1.0949	0.2139	0.9873	0.5099	0.9994	13.3901	1.0949	5	0.7032
795283	0.0861	0.9968	5.3079	1.0043	0.0857	0.9921	0.2019	1.0057	5.3093	1.0043	6	0.7033

Table 5.2: Test 2: convergence history and Newton iteration count for the $\mathbb{P}_k - \mathbb{RT}_k - \mathbf{P}_{k+1}$ approximations of the Navier-Stokes problem with $k = 0$, and convergence of the postprocessed pressure field. Values computed under uniform (top rows) and adaptive (bottom) refinement.

Test 1. Our first example concentrates on the accuracy of the augmented method when a manufactured solution of (2.7) is given by the smooth functions

$$\boldsymbol{u} = \begin{pmatrix} -\cos(\pi x_1)\sin(\pi x_2) \\ \sin(\pi x_1)\cos(\pi x_2) \end{pmatrix}, \ \boldsymbol{t} = \nabla \boldsymbol{u}, \ \tilde{\boldsymbol{\sigma}} = \mu(|\nabla \boldsymbol{u}|)\nabla \boldsymbol{u} - \boldsymbol{u} \otimes \boldsymbol{u} - (x_1^2 - x_2^2)\mathbb{I}, \ \boldsymbol{\sigma} = \tilde{\boldsymbol{\sigma}} - \frac{1}{8}(\int_\Omega \mathrm{tr}\tilde{\boldsymbol{\sigma}})\mathbb{I},$$

defined on the square domain $\Omega = (-1, 1)^2$. The external load $\boldsymbol{f}$ and the boundary datum $\boldsymbol{g}$ are determined from these solutions. The viscosity parameters are set as $\alpha_0 = 3$, $\alpha_1 = 4$. A sequence of successively refined uniform triangulations of the domain is used to present the error history displayed in Table 5.1. Discrete norms and the convergence rate between two consecutive meshes of size h and $\hat{h}$ are defined as

$$e(\boldsymbol{t}) = \|\boldsymbol{t} - \boldsymbol{t}_h\|_{0,\Omega}, \ e(\boldsymbol{\sigma}) = \|\boldsymbol{\sigma} - \boldsymbol{\sigma}_h\|_{\mathbf{div},\Omega}, \ e(\boldsymbol{u}) = \|\boldsymbol{u} - \boldsymbol{u}_h\|_{1,\Omega}, \ r(\cdot) = \log(e(\cdot)/\hat{e}(\cdot))[\log(h/\hat{h})]^{-1}.$$

The results reported in Table 5.1 are in accordance with the theoretical bounds established in Theorem 2.3. In addition, we also compute the global a posteriori error indicators $\boldsymbol{\theta}_1$, $\boldsymbol{\theta}_2$ and measure their reliability and efficiency with the efficiency index. For the two orders tested, these estimators remain always bounded. The approximate solutions computed with $k = 1$ are displayed in Figure 5.1.

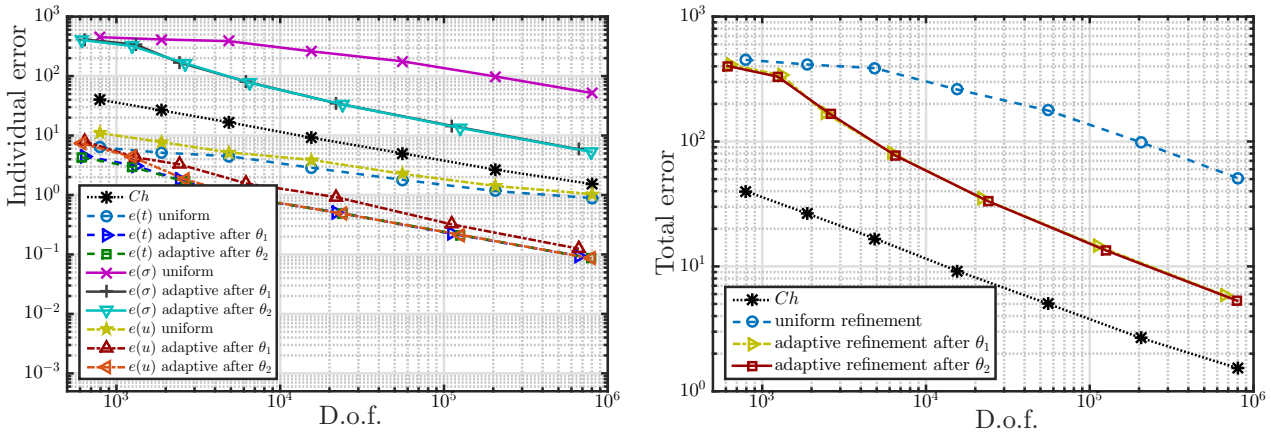

Figure 5.2: Test 2: Convergence test against analytical solutions employing the lowest order family $k = 0$. Individual contributions (left) and global errors (right) computed on a sequence of uniformly and adaptively refined meshes according to the a posteriori error estimators $\boldsymbol{\theta}_1$ and $\boldsymbol{\theta}_2$.

Test 2. Our next numerical experiment is aimed at testing the features of adaptive mesh refinement after the a posteriori error estimators $\boldsymbol{\theta}_1, \boldsymbol{\theta}_2$. Removing the unit square from the computational domain considered in Test 1 we end up with an L-shaped domain $\Omega = (-1, 1)^2 \setminus [0, 1]^2$. Let us further consider the same exact velocity and velocity gradient as in Test 1, but now the volumetric part of the Cauchy stress (the pressure field) assumes a different expression, yielding

$$\tilde{\boldsymbol{\sigma}} = \mu(|\nabla \boldsymbol{u}|)\nabla \boldsymbol{u} - \boldsymbol{u} \otimes \boldsymbol{u} - (1 - x_1)\big[(x_1 - 1/20)^2 + (x_2 - 1/20)^2\big]^{-1}\mathbb{I}.$$

Under uniform refinement, a hampering of the convergence rates is expected due to the stress singularity near the origin (where the domain has a reentrant corner).

For Tests 2 and 3 we compute individual convergence rates as

$$r(\cdot) := -2\log(e(\cdot)/\hat{e}(\cdot))[\log(N/\hat{N})]^{-1},$$

where N and $\hat{N}$ denote the corresponding degrees of freedom at each triangulation, and we also define the total error, its convergence rate, and the effectivity index associated to the scheme where the mesh refinement has been applied according to a given global estimator $\boldsymbol{\theta}_i$, $i \in \{1, 2\}$ as

$$\mathtt{e} := \big\{[e(\boldsymbol{t})]^2 + [e(\boldsymbol{\sigma})]^2 + [e(\boldsymbol{u})]^2\big\}^{1/2}, \quad \mathtt{r} := -2\log(\mathtt{e}/\hat{\mathtt{e}})[\log(N/\hat{N})]^{-1}, \quad \mathtt{eff}(\boldsymbol{\theta}_i) := \mathtt{e}\,\boldsymbol{\theta}_i^{-1}.$$

We carry out a classical adaptive mesh refinement based on the equi-distribution of the local error indicators: the diameter of each element in the new fine mesh, which is contained in a generic element T on the initial coarse mesh, is proportional to the diameter of the old element times the ratio $\frac{\tilde{\theta}_i}{\theta_{i,T}}$, where $\tilde{\theta}_i$ stands for the average of θ_i over the old triangulation (cf. [38]).

Table 5.2 along with Figure 5.2 report on the error history under uniform and adaptive refinement. Sub-optimal rates are observed in the first case (not only for the total error, but for each field), whereas adaptive refinement according to either a posteriori error indicator yield optimal convergence and stable effectivity indexes. Notice also that, even if the total errors have practically the same rate of convergence and the same orders of magnitude for both error estimators, $\boldsymbol{\theta}_2$ delivers lower errors for the velocity. Approximate solutions computed with an augmented $\mathbb{P}_0 - \mathbb{RT}_0 - \mathbf{P}_1$ family are

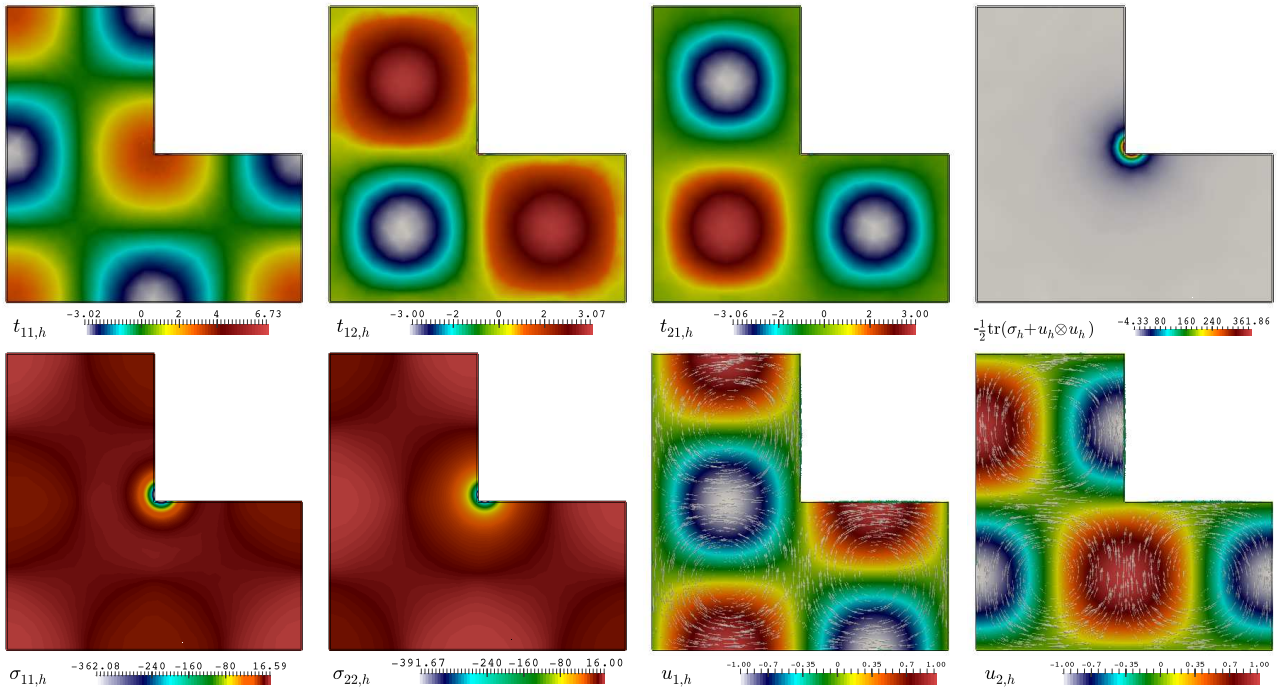

Figure 5.3: Test 2: Approximate solutions computed with a lowest order family $k = 0$.

shown in Figure 5.3, and examples of some adapted meshes generated using $\boldsymbol{\theta}_1$ and $\boldsymbol{\theta}_2$ are collected in Figure 5.4. We can observe a clear clustering of elements near the reentrant corner (where pressure and stresses exhibit high gradients), and also in the zones where the pseudo-stress and the viscosity show sharp profiles.

Test 3. To conclude, we replicate Test 2 in a three-dimensional setting. This time the manufactured exact solutions adopt the form

$$\boldsymbol{u} = \begin{pmatrix} \cos(x_1)\sin(x_2)\sin(x_3) \\ \sin(x_1)\cos(x_2)\sin(x_3) \\ -2\sin(x_1)\sin(x_2)\cos(x_3) \end{pmatrix}, \qquad \boldsymbol{t} = \nabla\boldsymbol{u},$$

$$\tilde{\boldsymbol{\sigma}} = \mu(|\nabla\boldsymbol{u}|)\nabla\boldsymbol{u} - \boldsymbol{u}\otimes\boldsymbol{u} - (1 - x_1^2 - x_2^2 - x_3^2)\big[(x_1 - 1/20)^2 + (x_2 - 1/20)^2 + (x_3 - 1.01)^2\big]^{-1}\mathbb{I},$$

and the domain consists on the polygon $\Omega = \Big((-1,1)^2 \setminus [0,1]^2\Big) \times (0,1)$, so $\boldsymbol{\sigma} = \tilde{\boldsymbol{\sigma}} - \frac{1}{9}(\int_\Omega \mathrm{tr}\tilde{\boldsymbol{\sigma}})\mathbb{I}$. All remaining parameters and functions are taken as in the previous test. Again, from the computations we observe a disturbed convergence under uniform refinement, and we confirm the recovering of optimal convergence rates when using adaptive refinement guided by the a posteriori error estimator $\boldsymbol{\theta}_1$ (see a summary in Table 5.3). Resulting approximations after five mesh refinement steps are collected in Figure 5.5, whereas snapshots of intermediate meshes are shown in Figure 5.6.

References

[1] R.A. Adams and J.J.F. Fournier, *Sobolev Spaces*. Second edition. Pure and Applied Mathematics (Amsterdam), 140. Elsevier/Academic Press, Amsterdam, 2003.

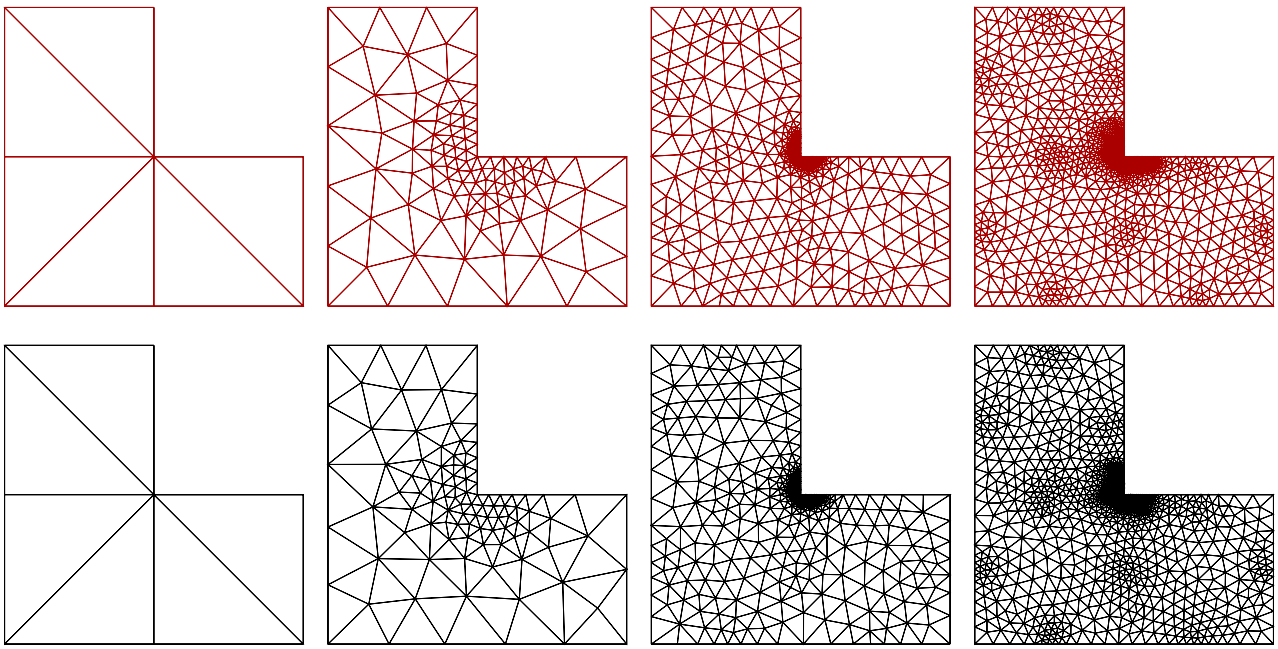

Figure 5.4: Test 2: Four snapshots of successively refined meshes according to the indicators $\boldsymbol{\theta}_1$ and $\boldsymbol{\theta}_2$ (top and bottom panels, respectively).

D.o.f.	h	$e(\boldsymbol{t})$	$r(\boldsymbol{t})$	$e(\boldsymbol{\sigma})$	$r(\boldsymbol{\sigma})$	$e(\boldsymbol{u})$	$r(\boldsymbol{u})$	$e(p)$	$r(p)$	iter	$\texttt{eff}(\boldsymbol{\theta}_1)$
780	1.4142	10.9909	–	263.6320	–	19.0890	–	9.9553	–	8	0.9704
5292	0.9100	7.9574	0.4374	152.8142	0.5851	11.2698	0.5505	7.6034	0.4049	7	0.9651
76245	0.4445	4.0528	0.6058	106.9313	0.6097	5.2593	0.5714	3.7098	0.6822	7	0.9614
185783	0.3256	3.2810	0.7197	84.2115	0.7066	3.9306	0.6843	2.5122	0.8245	8	0.9622
507525	0.2578	2.2585	0.8769	58.0277	0.8752	2.6238	0.8195	1.3252	1.0972	7	0.9628
2032544	0.1631	1.0433	0.9586	36.8432	0.9731	1.0456	0.9366	0.5893	1.0095	7	0.9633

Table 5.3: Test 3: individual errors and Newton iteration count for the $\mathbb{P}_0 - \mathbb{RT}_0 - \mathbf{P}_1$ approximations of the Navier-Stokes equations. Values computed under adaptive refinement guided by $\boldsymbol{\theta}_1$.

[2] S. Agmon, Lectures on Elliptic Boundary Value Problems. Van Nostrand, Princeton, New Jersey, 1965.

[3] M. Ainsworth and J.T. Oden, *A posteriori error estimation in finite element analysis*. Comput. Methods Appl. Mech. Engrg. 142 (1997), no. 1-2, 1–88.

[4] M. Alvarez, G. N. Gatica and R. Ruiz-Baier, *A posteriori error analysis for a viscous flow – transport problem*. ESAIM: Math. Model. Numer. Anal. DOI:10.1051/m2an/2016007.

[5] C. Amrouche, C. Bernardi, M. Dauge and V. Girault, *Vector potentials in three-dimensional non-smooth domains*. Math. Methods Appl. Sci. 21 (1998), no. 9, 823–864.

[6] D. Arnica and C. Padra, *A posteriori error estimators for the steady incompressible Navier-Stokes equations*. Numer. Methods Partial Differential Equations 13 (1997), no. 5, 561–574.

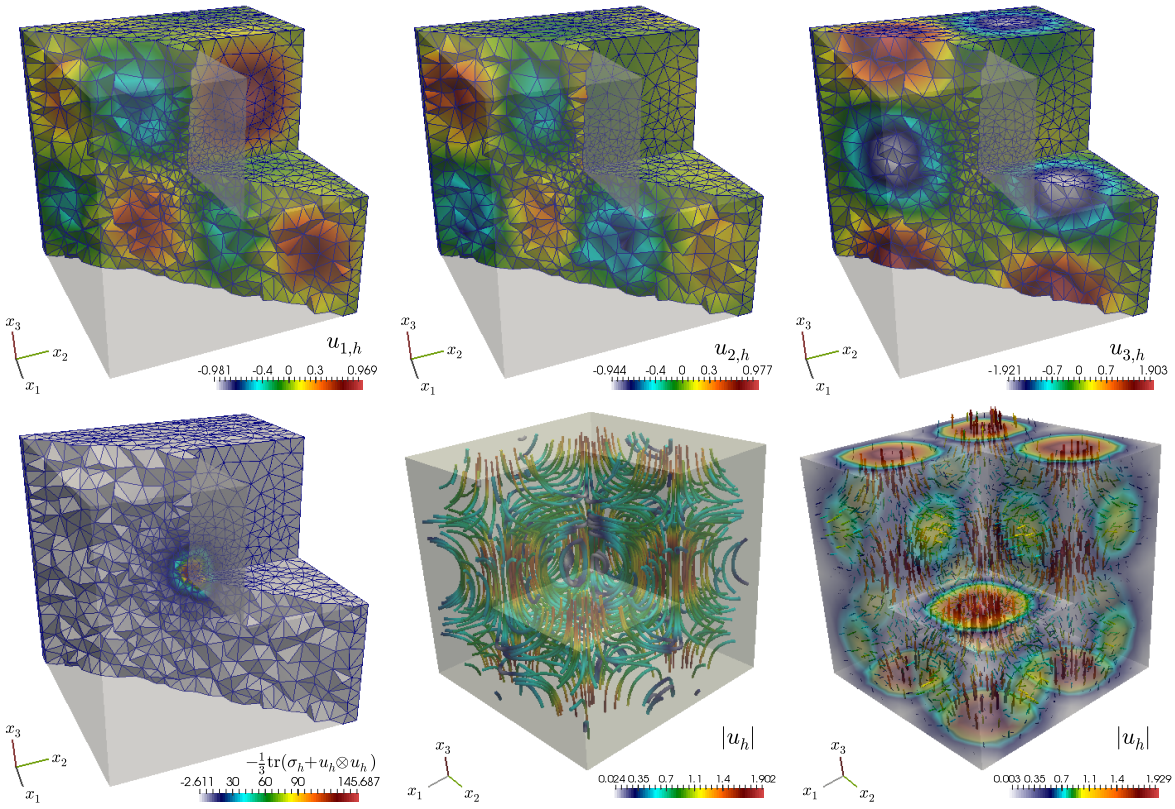

Figure 5.5: Test 3: approximate numerical solutions computed with the lowest order method on a mesh adapted after the first estimator $\boldsymbol{\theta}_1$.

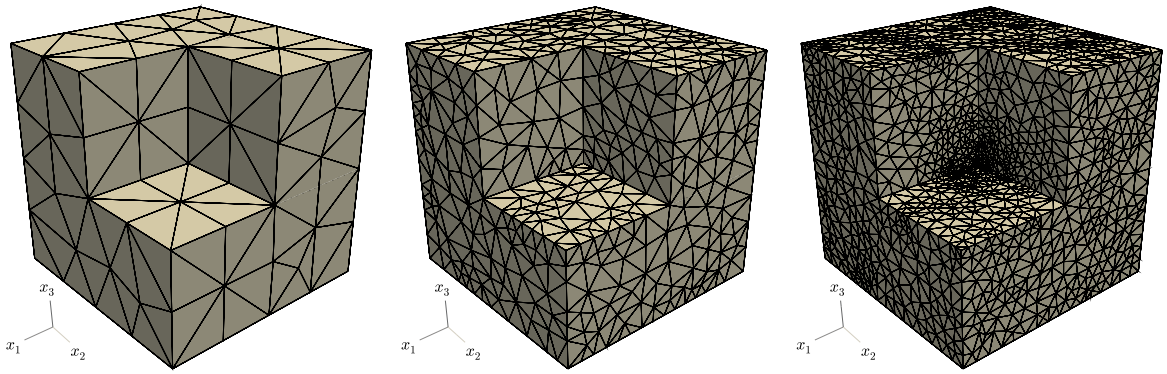

Figure 5.6: Test 3: three snapshots of successively refined meshes according to the indicator $\boldsymbol{\theta}_1$.

[7] T.P. Barrios, G.N. Gatica, M. González and N. Heuer, *A residual based a posteriori error estimator for an augmented mixed finite element method in linear elasticity.* ESAIM: Math. Model. Numer. Anal. 40 (2006), no. 5, 843–869 (2007).

[8] R. Becker, *An optimal-control approach to a posteriori error estimation for finite element discretizations of the Navier-Stokes equations.* East-West J. Numer. Math. 8 (2000), no. 4, 257–274.

[9] C. Bernardi, J. Dakroub, G. Mansour and T. Sayah, *A posteriori analysis of an iterative algorithm for Navier-Stokes problem*. ESAIM: Math. Model. Numer. Anal. DOI:10.1051/m2an/2015062

[10] C. Bernardi and T. Sayah, *A posteriori error analysis of the time dependent Navier–Stokes equations with mixed boundary conditions*. SēMA J. 69 (2015), 1–23.

[11] J. Camaño, G.N. Gatica, R. Oyarzúa and G. Tierra, *An augmented mixed finite element method for the Navier-Stokes equations with variable viscosity*. SIAM J. Numer. Anal. 54 (2016), no. 2, 1069–1092.

[12] J. Camaño, R. Oyarzúa and G. Tierra, *Analysis of an augmented mixed-FEM for the Navier Stokes problem*. Math. Comp., to appear.

[13] C. Carstensen, *A-posteriori error estimate for the mixed finite element method*. Math. Comp. 66 (1997), no. 218, 465–476.

[14] P.G. Ciarlet, The Finite Element Method for Elliptic Problems. North-Holland, Amsterdam, New York, Oxford, 1978.

[15] P. Clément, *Approximation by finite element functions using local regularisation*. RAIRO Analyse Numérique 9 (1975), no. R-2, 77–84.

[16] J. De Frutos, B. García-Archilla and J. Novo, *A posteriori error estimations for mixed finite-element approximations to the Navier-Stokes equations*. J. Comput. Appl. Math. 236 (2011), no. 6, 1103–1122.

[17] C. Domínguez, G.N. Gatica and S. Meddahi, *A posteriori error analysis of a fully-mixed finite element method for a two-dimensional fluid-solid interaction problem*. J. Comput. Math. 33 (2015), no. 6, 606–641.

[18] A. Ern and J.-L. Guermond, Theory and Practice of Finite Elements. Applied Mathematical Sciences, 159. Springer-Verlag, New York, 2004.

[19] M. Farhloul, S. Nicaise and L. Paquet, *A posteriori error estimation for the dual mixed finite element method of the Stokes problem*. Numer. Funct. Anal. Optim. 27 (2006), no. 7-8, 831–846.

[20] M. Farhloul, S. Nicaise and L. Paquet, *A priori and a posteriori error estimations for the dual mixed finite element method of the Navier-Stokes problem*. Numer. Methods Partial Differential Equations 25 (2009), no. 4, 843–869.

[21] A.I. Garralda-Guillem, M. Ruiz-Galán, G.N. Gatica and A. Márquez, *A posteriori error analysis of twofold saddle point variational formulations for nonlinear boundary value problems*. IMA J. Numer. Anal. 34 (2014), no. 1, 326–361.

[22] G.N. Gatica, A Simple Introduction to the Mixed Finite Element Method: Theory and Applications. Springer Briefs in Mathematics. Springer, Cham, 2014.

[23] G.N. Gatica, *A note on stable Helmholtz decompositions in* 3D. Preprint 2016-03, Centro de Investigación en Ingeniería Matemática (CI^{2}MA), Universidad de Concepción, Chile, 2016 [available at `http://www.ci2ma.udec.cl/publicaciones/prepublicaciones`].

[24] G.N. Gatica, L.F. Gatica, and A. Márquez, *Analysis of a pseudostress-based mixed finite element method for the Brinkman model of porous media flow*. Numer. Math. 126 (2014), no. 4, 635–677.

[25] G.N. Gatica, L.F. Gatica, and F. Sequeira, *A priori and a posteriori error analyses of a pseudostress-based mixed formulation for linear elasticity*. Comput. Mat. Appl. 71 (2016), no. 2, 585–614.

[26] G.N. Gatica, A. Márquez and M.A. Sánchez, *Analysis of a velocity-pressure-pseudostress formulation for the stationary Stokes equations*. Comput. Methods Appl. Mech. Engrg. 199 (2010), no. 17-20, 1064–1079.

[27] G.N. Gatica, A. Márquez and M.A. Sánchez, *A priori and a posteriori error analyses of a velocity-pseudostress formulation for a class of quasi-Newtonian Stokes flows*. Comput. Methods Appl. Mech. Engrg. 200 (2011), no. 17-20, 1619–1636.

[28] G.N. Gatica and W. Wendland, *Coupling of mixed finite elements and boundary elements for linear and nonlinear elliptic problems*. Appl. Anal. 63 (1996), no. 1-2, 39–75.

[29] V. Girault and P.-A. Raviart, Finite Element Methods for Navier-Stokes Equations. Theory and Algorithms. Springer Series in Computational Mathematics, 5. Springer-Verlag, Berlin, 1986.

[30] R. Hartmann and P. Houston, *Symmetric interior penalty DG methods for the compressible Navier-Stokes equations*. II. *Goal-oriented a posteriori error estimation*. Int. J. Numer. Anal. Model. 3 (2006), no. 2, 141–162.

[31] G. Kanschat and D. Schötzau, *Energy norm a posteriori error estimation for divergence-free discontinuous Galerkin approximations of the Navier-Stokes equations*. Int. J. Numer. Methods Fluids 57 (2008), no. 9, 1093–1113.

[32] J.S. Howell and N.J. Walkington, *Dual-mixed finite element methods for the Navier-Stokes equations*. ESAIM Math. Model. Numer. Anal. 47 (2013), no. 3, 789–805.

[33] G. Lei, T. Zhang and X. Zhao, *A posteriori error estimates of stabilized finite element method for the steady Navier-Stokes problem*. Appl. Math. Comput. 219 (2013), no. 17, 9081–9092.

[34] J.T. Oden, L. Demkowicz, W. Rachowicz and T.A. Westermann, *A posteriori error analysis in finite elements: the element residual method for symmetrizable problems with applications to compressible Euler and Navier-Stokes equations*. Reliability in Computational Mechanics (Austin, TX, 1989). Comput. Methods Appl. Mech. Engrg. 82 (1990), no. 1-3, 183–203.

[35] J.T. Oden, W. Wu and M. Ainsworth, *An a posteriori error estimate for finite element approximations of the Navier-Stokes equations*. Comput. Methods Appl. Mech. Engrg. 111 (1994), no. 1-2, 185–202.

[36] A. Quarteroni and A. Valli, Numerical Approximation of Partial Differential Equations. Springer Series in Computational Mathematics, 23. Springer-Verlag, Berlin, 1994.

[37] S. Repin, *On a posteriori error estimates for the stationary Navier-Stokes problem*. Problems in mathematical analysis. No. 36. J. Math. Sci. (N. Y.) 150 (2008), no. 1, 1885–1889.

[38] R. Verfürth, A Review of A-Posteriori Error Estimation and Adaptive Mesh-Refinement Techniques. John Wiley and Teubner Series. Advances in Numerical Mathematics, 1996.

[39] R. Verfürth, *A posteriori error estimators and adaptive mesh-refinement techniques for the Navier-Stokes equations*. Incompressible computational fluid dynamics: trends and advances, 447–475, Cambridge Univ. Press, Cambridge, 2008.

[40] R. Verfürth, A Posteriori Error Estimation Techniques for Finite Element Methods. Oxford University Press, 2013.